Competing hyperfine and spin-orbit couplings: Spin relaxation in a quantum Hall ferromagnet

S. Dickmann[1,2] and T. Ziman[2]

[1]*Institute for Solid State Physics of RAS, Chernogolovka 142432, Moscow District, Russia*

[2]*CNRS and Institut Laue Langevin, 6 rue Jules Horowitz, BP 156, F-38042 Grenoble, France*

(Received 13 October 2011; revised manuscript received 18 December 2011; published 18 January 2012)

Spin relaxation in a quantum Hall ferromagnet, where filling is $\nu = 1, 1/3, 1/5, \ldots$, can be considered in terms of spin-wave annihilation/creation processes. Hyperfine coupling with the nuclei of the GaAs matrix provides spin nonconservation in the two-dimensional electron gas and determines spin relaxation in the quantum Hall system. This mechanism competes with spin-orbit coupling channels of spin-wave decay and can even dominate in a low-temperature regime where T is much smaller than the Zeeman gap. In this case the spin-wave relaxation process occurs nonexponentially with time and does not depend on the temperature. The competition of different relaxation channels results in crossovers in the dominant mechanism, leading to nonmonotonic behavior of the characteristic relaxation time with the magnetic field. We predict that the relaxation times should reach maxima at $B \simeq 18$ T in the $\nu = 1$ quantum Hall system and at $B \simeq 12$ T for that of $\nu = 1/3$. We estimate these times as $\sim$10–30 μs and $\sim$2–5 μs, respectively.

DOI: 10.1103/PhysRevB.85.045318 PACS number(s): 73.43.Lp, 78.67.De, 73.21.Fg

I. INTRODUCTION

Two-dimensional (2D) electron gas has been intensively studied for several decades. The interest is stimulated by the clear manifestations of strong electron correlations, including quantum phase transitions (like Wigner crystallization[1]) and, in the presence of a strong perpendicular magnetic field, to various features in electron transport gathered under the name "fractional quantum Hall effect".[2] Transport phenomena, although of paramount significance for applications, provide only indirect information on such fundamental characteristics as quantum states and the energy spectrum, where optical techniques give much more immediate information. In particular, Raman scattering, starting from the pioneering works of A. Pinczuk *et al.*,[3] has been successfully used to study collective excitations in two-dimensional electron gas created in semiconductor heterostructures and quantum wells (see also Ref. 4 and references therein). The position and intensities of corresponding Raman or luminescence lines can yield information on the energy and oscillator strengths of the excited states. Meanwhile an important characteristic of such excitations is also the lifetime. This may be estimated by observation of the resonance linewidths: for example, the spin-wave lifetime was deduced from the observed width of the electron spin resonance lines.[5] Microwave and optical linewidths are not, however, directly related to the lifetime and usually provide only a very rough lower bound for this quantity. In consequence, one is forced to use combined experimental methods, including a time-resolved technique (see, e.g., Ref. 6). Despite these experimental difficulties, growing interest in the problem of excitation lifetimes in a two-dimensional electron gas has been observed in recent years. One should mention, for example, recent experimental works on the observation of the spin relaxation in a polarized two-dimensional electron gas based on the Kerr rotation effect.[7]

We study in this work the so-called quantum Hall ferromagnet where all two-dimensional electron gas electrons of the upper, partially filled Landau level, are in the ground state, with spins aligned along the magnetic field. This state obviously arises at odd integer fillings: $\nu = 1, 3, \ldots$.[8] In addition, experiments and semiphenomenological theories show that at some fractional fillings, namely at $\nu = 1/3, 1/5, \ldots$, electrons in the ground state occupy only one spin sublevel, and thereby the fractional quantum Hall ferromagnet state is also realized.[9–13] The quantum Hall ferromagnet possesses a macroscopically large spin $\vec{S}$ oriented in the direction of the field $\vec{B}$ due to negative g factor in GaAs structures. The spin wave in the quantum Hall ferromagnet may be defined as a purely electronic collective excitation within the Landau level which corresponds to a change of the spin numbers by 1,

$$\delta S = \delta S_z = -1, \tag{1.1}$$

and does not alter the spin *orientation* of the system. (Another possible excitation in the quantum Hall ferromagnet is a Goldstone mode representing a deviation of $\vec{S}$ from the $\vec{B}$ direction which does not change the S number;[14] the microscopic excitation then would be a "zero spin-exciton" corresponding to the spin change $\delta S_z = -1$, but $\delta S = 0$.) This spin wave is also called the spin exciton, because this excitation promotes an electron to another spin sublevel of the same Landau level and, thus, an effective hole appears in the initial sublevel. Every spin exciton possesses energy[8,10]

$$E_x = \epsilon_Z + \mathcal{E}_q, \tag{1.2}$$

where $\epsilon_Z = |g|\mu_B B$ is the Zeeman gap ($g \approx -0.44$ in a GaAs structure) and $\mathcal{E}_q$ is the spin-exciton Coulomb correlation energy depending on the 2D wave-vector modulus q. For the rest of the paper it will be sufficient to consider only long-wave excitations, $q \ll 1/l_B$ (l_B is the magnetic length), for which the spectrum is quadratic:

$$\mathcal{E}_q \approx q^2 l_B^2 / 2M_x. \tag{1.3}$$

Here the spin-exciton mass M_x has the dimensionality of inverse energy.[8,10] This quantity has recently been measured experimentally for $\nu = 1$[15,16] and $\nu = 1/3$ fillings.[11]

If there are an excessive number of spin excitons compared with equilibrium, then the spin relaxation reduces to an

elementary process of spin-exciton annihilation. The spin numbers are changed in accordance with Eq. (1.1), where the energy of the annihilated excitation can be transferred to the emitted acoustic phonon or to another exciton due to the spin-exciton–spin-exciton scattering. Any spin-exciton relaxation channel is, thus, determined by two necessary conditions: by the availability of an interaction that does not conserve the spin of the electron gas and by a mechanism of energy dissipation making the relaxation process irreversible. Until now, spin-orbit coupling has been assumed to be the cause of the spin nonconservation (see, e.g., Refs. 14 and 17 and the works cited therein). Indeed, these spin-orbit relaxation channels are certainly dominant under the usual experimental conditions, where $T \sim 1$ K and $1 < B < 10$ T. The corresponding calculations are in satisfactory agreement with the available experimental data. Here we shall extend the study of spin relaxation channels to include spin nonconservation by the hyperfine coupling to nuclei of the GaAs matrix. This has been considered previously[18] only for the case of the Goldstone mode $q \equiv 0$; here we consider nonzero, but small, q. Our analysis shows that one mechanism in particular, relating to the spin-exciton–spin-exciton scattering process, should be taken into account, if $T \lesssim 0.1$ K and magnetic fields $B \gtrsim 10$ T.[18] (Specifically, the necessary condition is $T \ll \epsilon_Z$.) To see this clearly we will analyze the spin-orbit relaxation channels; two of them can compete with the hyperfine coupling relaxation in the same region of temperature and magnetic fields.

It should also be noted that the spin relaxation processes proceed much more slowly than other two-dimensional electron gas plasma relaxations unrelated to a spin change. This means that, in any case, an elementary spin-exciton annihilation/creation process may be studied as a transition (induced by a perturbation) from an initial eigenstate $|i\rangle$ to a final eigenstate $|f\rangle$; i.e., the hyperfine coupling relaxation mechanisms are governed, like the spin-orbit coupling relaxation,[14,17,19–21] by the Fermi golden rule probability

$$w_{fi} = (2\pi/\hbar)|\mathcal{M}_{fi}|^2 \delta(E_f - E_i), \tag{1.4}$$

where $\mathcal{M}_{fi}$ is a relevant matrix element.

In principle, the hyperfine coupling effects are weak. The spin-orbit coupling and the hyperfine coupling both have relativistic origins: the former is of the first order, but the latter represents the second-order relativistic correction to the Hamiltonian. However, the hyperfine interaction has some essential properties differenting from those of the spin-orbit coupling. These substantially change kinematic conditions of the spin-exciton scattering and the dissipation mechanisms where one of the spin excitons annihilates. We shall see that, (i) first, the hyperfine coupling does not conserve total momentum of the electron system, and this feature leads to extension of the phase volume for the spin-exciton–spin-exciton and spin-exciton–phonon scatterings; and (ii) second, the spin-flip process governed be the hyperfine interaction does not require a virtual promotion of an electron to another Landau level (this promotion with simultaneous spin flip is a characteristic feature of the spin-orbit coupling and means a virtual conversion of the spin exciton into the cyclotron magnetoplasmon). As a result, a new annihilation channel of the spin-exciton scattering appears: two spin excitons can be

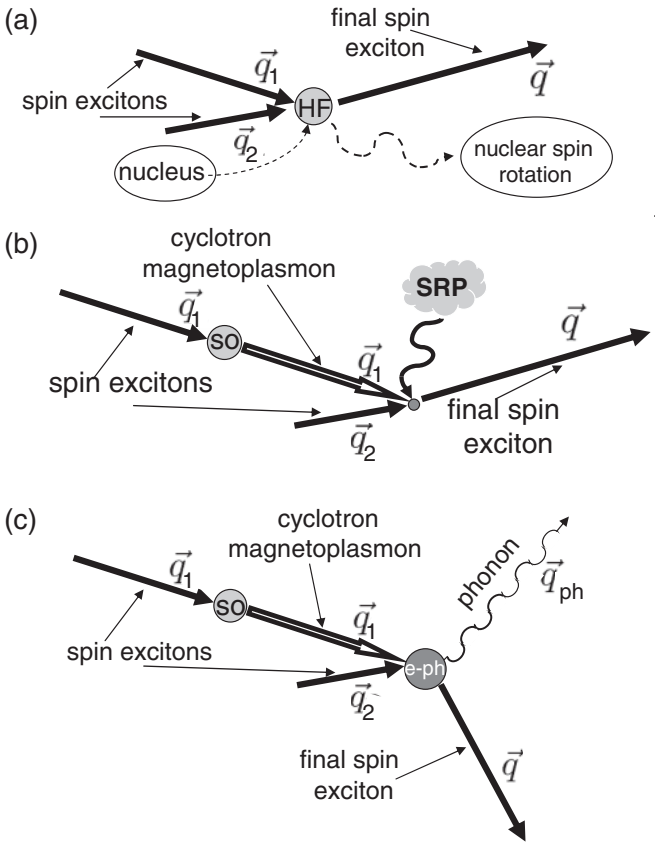

FIG. 1. Three diagrams illustrating the main elementary processes contributing to the spin relaxation rate. Spin excitons are depicted by bold arrows. (a) Scattering via hyperfine coupling to nuclei. (b) Scattering via spin-orbit coupling and coupling to an external disorder field modelled by a smooth random potential. (c) Scattering via spin-orbit coupling and coupling to phonons. Outlined arrows denote a virtual magnetoplasmon. For more details; see the text.

scattered by each other, within the same Landau level, directly due to the hyperfine interaction and one finally gets a single-spin-exciton state possessing the combined energy. This kind of scattering, as in the case of scattering caused by disorder,[14,17] is kinematic: The transition matrix element does not contain the Coulomb constant between bra and ket vectors. The scattering is possible because the spin excitons are not actually elementary Bose particles but possess an internal degree of freedom and, thus, have a "memory" of the Pauli principle for the primary electron system. Thus, in spite of the small hyperfine coupling constant, the hyperfine coupling channel competes with the spin-orbit ones and can even dominate.

The diagrams in Fig. 1 illustrate the main elementary processes that compete with one another and contribute to a combined spin-exciton relaxation rate. All three represent a two-spin-exciton scattering. The necessity of having two spin excitons in the initial state (and a single one in the final state) is determined by the energy conservation law for scattering by nuclei [Fig. 1(a) or via an external smooth random potential [Fig. 1(b)]. In the case of scattering via the electron-phonon (e-ph) coupling, a single-spin-exciton annihilation would also be possible.[17,20] However, this elementary process, where the energy and momentum of the spin exciton would be transferred to the generated phonon, would have a very small phase

volume, as compared with the two-spin-exciton scattering, for conditions where there is an appreciable density of optically excited spin excitons. So the third diagram [Fig. 1(c)] represents the most intense process where irreversibility occurs due to the electron-phonon coupling. The diagram in Fig. 1(a) shows the scattering by nuclei provided only by a *single* vertex corresponding to the hyperfine (HF) coupling. This diagram describes both kinematic and dynamic scatterings of spin excitons, where in the final state one has a single spin exciton with combined energy and a nuclear spin rotation, with change of the nuclear spin by $\delta I_z = 1$. Scattering processes in the diagrams of Figs. 1(b) and 1(c) are governed by two vertices, the first of which represents the spin-orbit (SO) coupling and provides a *virtual* transformation of one initial spin exciton into a purely orbital cyclotron exciton (magnetoplasmon) with the same wave vector. The second vertex is the coupling to the smooth random potential ["SRP" in Fig. 1(b)] or to phonons. (The latter is renormalized as a spin-exciton–phonon interaction.) In the case of scattering with participation of phonons [Fig. 1(c)], the combined energy of the two scattering spin excitons is passed to a final spin exciton and the generated phonon. Momentum conservation requires $\mathbf{q}_1 + \mathbf{q}_2 = \mathbf{q} + \mathbf{q}_{\rm ph}$, where $\mathbf{q}_{\rm ph}$ is the component of the phonon momentum in the (x, y) plane and $\mathbf{q}_1$, $\mathbf{q}_2$, and $\mathbf{q}$ are momenta of the spin excitons. In the case of scattering by a smooth random potential, the total combined energy is transferred to the final spin exciton, but there is no momentum conservation: $\mathbf{q}_1 + \mathbf{q}_2 \neq \mathbf{q}$. Similarly, momentum is not conserved for the case of scattering by nuclei [Fig. 1(a)].

The next section of the paper is devoted to formal description of the system where we present the Hamiltonian and the basis of exciton states (excitonic representation). In Sec. III we study the hyperfine coupling relaxation mechanisms when the spin-exciton annihilation/creation is determined by the spin-exciton–spin-exciton scattering, including the kinematic and dynamic scattering channels [Fig. 1(a)]. For this process the relaxation rate is proportional to the spin-exciton number squared, and, therefore, the relaxation is nonexponential with time. (In principle, it becomes exponential when the spin-exciton number approaches its equilibrium value, but the final exponential stage cannot, in fact, be observed under the condition $T \ll \epsilon_Z$.) We discuss also in Sec. III possible relaxation processes related to the hyperfine coupling and phonon emission/absorption, comparing them with other relaxation mechanisms. Section IV is devoted to the spin-orbit relaxation channels relevant to the considered region of strong magnetic fields and low temperatures. These spin-orbit mechanisms are also related to the spin-exciton–spin-exciton scattering but are determined by two different dissipation processes:- via coupling to a smooth random potential [Fig. 1(b)] or coupling to phonons [Fig. 1(c)].

In Sec. V we discuss the results of our study. The main result consists of the interplay of different relaxation processes. We compare those due to the hyperfine coupling and spin-orbit interactions and, summing all relaxation channels, calculate the total characteristic inverse time. In this "interplay regime," where the spin-exciton–spin-exciton channels dominate, the relaxation occurs nonexponentially, and the effective relaxation time reaches its maximum ∼1–5 μs depending on the Landau level fillings. Nevertheless, the relevant region of parameters T and B is not too extreme and experimentally quite accessible.

Note that in this paper we do not study the situation where the Goldstone condensate of "zero spin excitons" arises,[14,18] i.e., where there would be a rotation of the *direction* but not a reduction in the *magnitude* of the total spin of the system. Here we consider instead relaxation where there are, at low temperatures, a bulk number of spin excitons arising from an intensive external (e.g., optical) excitation. The initial state at low temperatures should be described as a (metastable) "thermodynamic condensate" of spin waves with nonzero, but small, wave vectors limited by the uncertainty determined by disorder.[14] We think that such situation, where most of the spin-exciton annihilation/creation events happen within the thermodynamic condensate, is realizable experimentally.

II. FORMAL STATEMENT OF THE PROBLEM: THE HAMILTONIAN AND THE BASIS OF EXCITON STATES

Our system consists of two components: electrons belonging to the two-dimensional electron gas and nuclei of Ga and As atoms. In addition, we consider piezo- and deformation couplings of the 2D electron gas electrons to the lattice, which are reduced to electron-phonon interaction. So, the Hamiltonian used is as follows:

$$\hat{H} = \hat{H}_1 + \epsilon_Z \hat{S}_z + \hat{H}_{\rm int} + \sum_j \hat{H}^{(j)}_{\rm hf} + \sum_j \hat{H}^{(j)}_{e-{\rm ph}}, \quad (2.1)$$

where $\hat{H}_1 = \sum_j [\hat{\mathbf{q}}_j^2/2m_e^* + H^{(j)}_{\rm so}]$ is a single-electron Hamiltonian, including the spin-orbit coupling part ($\hat{\mathbf{q}} = -i\nabla + e\mathbf{A}/c\hbar$); $\hat{S}_z = \sum_j \hat{\sigma}_z^{(j)}/2$; subscript j labels the electrons. The third term describes Coulomb energy of the *e-e* interaction, the fourth is the hyperfine interaction of electrons with nuclei, and the fifth is the operator of the electron-phonon interaction. If one holds $H_{\rm so} = 0$, we can omit the orbital single-electron energy terms—all states relevant to our problem belong to the same Landau level and, therefore, have the same orbital energy equal to $\hbar\omega_c \nu \mathcal{N}_\phi$ (ω_c is the cyclotron frequency and $\mathcal{N}_\phi$ is the Landau level degeneracy). We ignore also the energy of nuclei which consists of the contribution due to their interaction independent of the electrons and of the nuclear Zeeman energy. Variations of both, associated with change of nuclear spins, are negligibly small due to the tiny nuclear magnetic momentum.

In the following three sections (II A, II B, and II C) we neglect the spin-orbit coupling. The spin-orbit Hamiltonian and spin-orbit corrections, written in terms of the representation used, will be given in the Sec. II D.

A. Electron system: Excitonic representation

We now present the basis set of states diagonalizing the first three terms of the Hamiltonian (2.1) to leading order in parameter $r_c = (\alpha e^2/\kappa l_B)/\hbar\omega_c$ considered to be small ($\alpha < 1$ is the averaged form factor arising due to finiteness of the 2D layer thickness; κ is the dielectric constant). We do this by analogy with previous works,[14,17,19–21] defining the spin-exciton creation operator[22]

$$\mathcal{Q}^\dagger_{ab\,\mathbf{q}} = \frac{1}{\sqrt{\mathcal{N}_\phi}} \sum_p e^{-iq_x p} b^\dagger_{p+\frac{q_y}{2}} a_{p-\frac{q_y}{2}}, \quad (2.2)$$

where a_p and b_p are the Fermi annihilation operators corresponding to electron states on the upper Landau level with spin up ($a = \uparrow$) and spin down ($b = \downarrow$), respectively. Index p marks intrinsic Landau level states which have wave functions $\psi_{np}(\mathbf{r}) = (2\pi\mathcal{N}_\phi)^{-1/4} e^{ipy}\varphi_n(p+x)$ in the Landau gauge. [$\varphi_n(x)$ is the oscillator function, where n is number of the upper partially filled Landau level; in Eq. (2.2) and everywhere below we measure length in the l_B units wave vectors in the $1/l_B$ ones.] In the *odd-integer quantum Hall regime*, operator (2.2) acting on the ground state yields the *eigenstate* of the first two terms of Eq. (2.1), namely

$$\left[\epsilon_Z \hat{S}_z + \hat{H}_{\rm int}, \mathcal{Q}^\dagger_{ab\,\mathbf{q}}\right]|0\rangle = (\epsilon_Z + \mathcal{E}_q)\mathcal{Q}^\dagger_{ab\,\mathbf{q}}|0\rangle, \qquad (2.3)$$

where $|0\rangle = |\overbrace{\uparrow,\uparrow,\ldots\uparrow}^{\mathcal{N}_\phi}\rangle$. This basic property of the exciton state, $\mathcal{Q}^\dagger_{ab\,\mathbf{q}}|0\rangle$, is asymptotically exact to first order in r_c. After the introduction of intrasublevel operators $\mathcal{A}^\dagger_{\mathbf{q}} = \mathcal{N}_\phi^{-1/2}\mathcal{Q}^\dagger_{aa\mathbf{q}}$ and $\mathcal{B}^\dagger_{\mathbf{q}} = \mathcal{N}_\phi^{-1/2}\mathcal{Q}^\dagger_{bb\mathbf{q}}$, we obtain a closed Lie algebra for these exciton operators.[23–25] The commutation identities needed in our case are

$$\begin{aligned}\left[\mathcal{Q}_{\mathbf{q}_1}, \mathcal{Q}^+_{\mathbf{q}_2}\right] &= e^{i(\mathbf{q}_1\times\mathbf{q}_2)_z/2}\mathcal{A}_{\mathbf{q}_1-\mathbf{q}_2} \\ &\quad - e^{-i(\mathbf{q}_1\times\mathbf{q}_2)_z/2}\mathcal{B}_{\mathbf{q}_1-\mathbf{q}_2}, \\ e^{-i(\mathbf{q}_1\times\mathbf{q}_2)_z/2}\left[\mathcal{A}^\dagger_{\mathbf{q}_1}, \mathcal{Q}^\dagger_{\mathbf{q}_2}\right] &= -e^{i(\mathbf{q}_1\times\mathbf{q}_2)_z/2}\left[\mathcal{B}^\dagger_{\mathbf{q}_1}, \mathcal{Q}^\dagger_{\mathbf{q}_2}\right] \\ &= -\mathcal{N}_\phi^{-1}\mathcal{Q}^\dagger_{\mathbf{q}_1+\mathbf{q}_2}. \end{aligned} \qquad (2.4)$$

(Here and below we omit the subscript ab at the $\mathcal{Q}$ operators.) Note that the commutation algebra [Eq. (2.4)] is neither purely fermionic nor bosonic.

The interaction Hamiltonian $\hat{H}_{\rm int} = \frac{1}{2}\int d\mathbf{r}_1 d\mathbf{r}_2\, \hat{\Psi}^\dagger(\mathbf{r}_2)\hat{\Psi}^\dagger(\mathbf{r}_1)U(\mathbf{r}_1-\mathbf{r}_2)\hat{\Psi}(\mathbf{r}_1)\hat{\Psi}(\mathbf{r}_2)$ may be expressed in terms of the exciton operators.[24,25] If we keep in $\hat{H}_{\rm int}$ only the terms relevant to our problem, it takes a very simple form,

$$\hat{H}_{\rm int} = \frac{\mathcal{N}_\phi}{2}\sum_{\mathbf{q}} W(q)(\mathcal{A}^\dagger_{\mathbf{q}}\mathcal{A}_{\mathbf{q}} + 2\mathcal{A}^\dagger_{\mathbf{q}}\mathcal{B}_{\mathbf{q}} + \mathcal{B}^\dagger_{\mathbf{q}}\mathcal{B}_{\mathbf{q}}), \qquad (2.5)$$

where $W(q) = U(q)[f(q)]^2$, where $f = e^{-q^2/4}$ if $\nu \leqslant 1$, or $f = e^{-q^2/4}[L_n(q^2/2)]$ if $\nu = 2n+1$ (L_n is the Laguerre polynomial). $U(q)$ is the Fourier component of the 2D Coulomb interaction function: $U(q) = (e^2/\kappa l_B q)\iint dz_1 dz_2 e^{-q|z_1-z_2|}|\chi(z_1)|^2|\chi(z_2)|^2$, where $\chi(z)$ is the dimensionally quantized wave function of an electron sized in the z direction.

In contrast to integer quantum Hall ferromagnet, the use of the excitonic basis $\mathcal{Q}^\dagger_{\mathbf{q}}|0\rangle$ presents only a *model approach* in the case of *fractional quantum Hall regime*. Generally, at fractional filling, spin-flip excitations within the same Landau level might have a many-particle rather than two-particle nature because the same change in the spin numbers [Eq. (1.1)] may be achieved with participation of arbitrary number of intra-spin-sublevel excitations (charge-density waves). These waves are generated by the operator $\mathcal{A}^\dagger_{\mathbf{q}}$ acting on the ground state $|0\rangle = |\overbrace{\uparrow,\ldots\uparrow,\ldots\uparrow}^{\nu\mathcal{N}_\phi}\rangle$.[9] The result is trivial in the case of integer ν ($\mathcal{A}^\dagger_{\mathbf{q}}|0\rangle = \delta_{\mathbf{q},0}|0\rangle$); however, states of the $\mathcal{Q}^\dagger_{\mathbf{q}_1}\mathcal{A}^\dagger_{\mathbf{q}_2}\mathcal{A}^\dagger_{\mathbf{q}_3}\ldots|0\rangle$ type might constitute a basis set if one studies the spin-flip process at fractional ν. On the other hand, a comprehensive phenomenological analysis[9,10] suggests that even the spin-flip basis reduced to single-mode (single-exciton) states would be quite appropriate, at least for the lowest-energy excitations in the case of fractional quantum Hall ferromagnet. This single-mode approach is indirectly substantiated by the fact that the charge-density wave has a Coulomb gap[9] which is substantially larger than the Zeeman gap ϵ_Z. Hence, for a fractional quantum Hall ferromagnet, just as in Ref. 10, we will consider the simple state $\mathcal{Q}^\dagger_{\mathbf{q}}|0\rangle$ to describe the spin-flip excitation. However, the calculation of $\langle 0|\mathcal{A}_{\mathbf{q}}\mathcal{A}^\dagger_{\mathbf{q}'}|0\rangle$ is required for the following. Now this expectation is not simply equal to $\delta_{\mathbf{q},0}\delta_{\mathbf{q}',0}$ but is expressed in terms of the two-particle correlation function $g(r)$ calculated for the ground state

$$\langle 0|\mathcal{A}_{\mathbf{q}}\mathcal{A}^\dagger_{\mathbf{q}'}|0\rangle = \frac{\nu}{\mathcal{N}_\phi}\left[2\pi\nu\overline{g}(q)e^{q^2/2}+1\right]\delta_{\mathbf{q}',\mathbf{q}} \quad (\nu \leqslant 1), \qquad (2.6)$$

where $\overline{g}(q) = \frac{1}{(2\pi)^2}\int g(r)e^{-i\mathbf{q}\mathbf{r}}d^2r$ is the Fourier component. The function $g(r)$ is known, e.g., in the case of Laughlin's state.[9,26] If the ground state is described by the Hartree-Fock approximation, we have simply $2\pi\overline{g} = (\mathcal{N}_\phi\delta_{q,0} - e^{-q^2/2})$, which does not depend on ν. Furthermore, at odd-integer filling factors this Hartree-Fock expression becomes a Fourier component of the *exact* correlation function. In the latter case one should also formally set $\nu = 1$ in Eq. (2.6). Note also that the exact equation $\langle 0|\mathcal{A}^\dagger_{\mathbf{q}}|0\rangle = \nu'\delta_{\mathbf{q},0}$ holds, where we set $\nu' = \nu$ if $\nu \leqslant 1$ but $\nu' = 1$ if $\nu = 3,5,\ldots$.

With the help of Eqs. (2.4) and (2.5) one can check Eq. (2.3) in the case of odd-integer ν. If ν is fractional, the Coulomb exciton energy within the single-mode approximation is defined as $\mathcal{E}_q = \langle 0|\mathcal{Q}_{\mathbf{q}}[\hat{H}_{\rm int}, \mathcal{Q}^\dagger_{\mathbf{q}}]|0\rangle / \langle 0|\mathcal{Q}_{\mathbf{q}}\mathcal{Q}^\dagger_{\mathbf{q}}|0\rangle$.[10] As a result in both cases of integer or fractional $\nu < 1$ one obtains for small q the quadratic dispersion law (1.3) with the spin-exciton mass

$$1/M_x = \frac{1}{2}\int_0^\infty W(q)q^3\left(1 - \frac{\mathcal{N}_\phi}{\nu'}\langle 0|\mathcal{A}_{\mathbf{q}}\mathcal{A}^\dagger_{\mathbf{q}}|0\rangle\right)dq. \qquad (2.7)$$

We have employed the rule for change from summation to integration over the 2D vector $\mathbf{q}$: $\sum_{\mathbf{q}}\ldots = \mathcal{N}_\phi\int\ldots\, qdqd\phi/2\pi$.

B. Hyperfine coupling

The general expression of the hyperfine coupling Hamiltonian[27] is simplified in the case of interaction with nuclei in a semiconductor matrix.[28–30] As this simplification is valid in the 2D channel of a quantum well we may directly start from the well-known expression for contact interactions of electrons with nuclei

$$\hat{H}_{\rm hf} = \frac{v_0}{2}\sum_n A_n\Psi^*(\boldsymbol{R}_n)(\hat{\boldsymbol{I}}^{(n)}\cdot\hat{\boldsymbol{\sigma}})\Psi(\boldsymbol{R}_n), \qquad (2.8)$$

(see, for example, Ref. 29 and references therein), where $\hat{\boldsymbol{I}}^{(n)}$ and $\boldsymbol{R}_n$ are spin and position of the nth nucleus and $\Psi(\boldsymbol{R})$ is the envelope function of electron [$\boldsymbol{R} = (\mathbf{r}, z)$ is the 3D vector]. Both Ga and As nuclei have the same total spin: $I^{\rm Ga} = I^{\rm As} = 3/2$. In Eq. (2.8) v_0 is the volume of the unit cell. The parameter A_n, being inversely proportional to v_0, really depends only on position of the Ga/As nucleus within the unit cell. For the final

calculation we need the sum $A_{\rm Ga}^2 + A_{\rm As}^2$. If v_0 is volume of the two atom unit cell, then $A_{\rm Ga}^2 + A_{\rm As}^2 \simeq 4 \times 10^{-3}$ meV^2 (see Appendix A).

We now rewrite $\hat{\boldsymbol{I}}^{(n)} \cdot \hat{\boldsymbol{\sigma}}$ as $\hat{I}_z\hat{\sigma}_z + \hat{I}_+\hat{\sigma}_- + \hat{I}_-\hat{\sigma}_+$. Then, omitting the $\hat{I}_z\hat{\sigma}_z$ term due to its irrelevance to any spin-flip process and substituting in Eq. (2.8) the Schrödinger operators $\hat{\Psi}^\dagger(\boldsymbol{R}) = \chi(z)\sum_p (a_p^\dagger + b_p^\dagger)\psi_p^*(\mathbf{r})$ and $\hat{\Psi}(\boldsymbol{R}) = (\hat{\Psi}^\dagger)^\dagger$ instead of Ψ^* and Ψ, we come to

$$\hat{H}_{\rm hf} = \frac{v_0}{2}\sum_{p_1,p_2} b_{p_2}^\dagger a_{p_1} \sum_n |\chi(Z_n)|^2 \psi_{p_2}^*(X_n,Y_n) \times \psi_{p_1}(X_n,Y_n) A_n \hat{I}_+^{(n)} + \text{H.c.}. \quad (2.9)$$

Substitution of the equation

$$b_{p_2}^\dagger a_{p_1} = \sum_{\mathbf{q}} \frac{e^{iq_x(p_2 - q_y/2)}}{\sqrt{\mathcal{N}_\phi}} \delta_{q_y, p_2 - p_1} \mathcal{Q}_{\mathbf{q}}^\dagger, \quad (2.10)$$

which is simply inverse to Eq. (2.2), yields, after summation over p_1 and p_2, the hyperfine coupling Hamiltonian in the excitonic representation:

$$\hat{H}_{\rm hf} = \frac{v_0}{4\pi l_B^2 \sqrt{\mathcal{N}_\phi}} \sum_{\mathbf{q}} f(q)\mathcal{Q}_{\mathbf{q}} \sum_n A_n |\chi(Z_n)|^2 \times e^{i\mathbf{q}\boldsymbol{R}_n} \hat{I}_-^{(n)} + \text{H.c.}. \quad (2.11)$$

A set of the I_z spin numbers $\{M\} = (M_1, M_2, \ldots M_n, \ldots)$, where every M_n may take on values $-3/2, -1/2, 1/2, 3/2$, completely determines the state of the nuclear system. The state where 2D electrons are in the ground state and nuclei in the state $\{M\}$ we denote as $|\{M\},0\rangle$. By applying the lowering/raising operator $I_\mp^{(n)}$ to this state, we obtain

$$\hat{I}_\mp^{(n)}|\{M\},0\rangle = \sqrt{\left(\frac{5}{2} \mp M_n\right)\left(\frac{3}{2} \pm M_n\right)}|\{M\}_n^\mp,0\rangle, \quad (2.12)$$

where $\{M\}_n^\mp = (M_1, M_2, \ldots M_n \mp 1, \ldots)$. Let us find the hyperfine coupling correction to the normalized spin-exciton state $\mathcal{Q}^\dagger|\{M\},0\rangle/\sqrt{\nu'}$. Considering operator (2.11) as a perturbation we obtain with the help of Eqs. (2.4) and (2.12):

$$|\text{SE},\mathbf{q}\rangle = \mathcal{Q}_{\mathbf{q}}^\dagger|\{M\},0\rangle/\sqrt{\nu'} + \frac{v_0\sqrt{\nu'}f(q)}{4\pi\sqrt{\mathcal{N}_\phi}l_B^2 E_{\rm x}(q)} \sum_n A_n|\chi(Z_n)|^2 e^{i\mathbf{q}\boldsymbol{R}_n} \times \sqrt{\left(\frac{5}{2} - M_n\right)\left(\frac{3}{2} + M_n\right)}|\{M\}_n^-,0\rangle. \quad (2.13)$$

In the same way we find the corrected nuclear "spin-turned" (NST) state

$$|\text{NST},n\rangle = |\{M\}_n^-,0\rangle - \frac{v_0}{4\pi\sqrt{\mathcal{N}_\phi}l_B^2}\sum_{\mathbf{q},n'} \frac{f(q)}{E_{\rm x}(q)} A_{n'}|\chi(Z_{n'})|^2 e^{-i\mathbf{q}\boldsymbol{R}_{n'}} \times \sqrt{\left(\frac{5}{2} + M_{n'} - \delta_{n',n}\right)\left(\frac{3}{2} - M_{n'} + \delta_{n',n}\right)}\mathcal{Q}_{\mathbf{q}}^\dagger|\{M\}_{nn'}^{-+},0\rangle, \quad (2.14)$$

where we consider $M_n > -3/2$, and use notation $\{M\}_{nn'}^{-+} = (M_1, \ldots M_n - 1, \ldots M_{n'} + 1, \ldots)$ meaning by that $\{M\}_{nn}^{-+} \equiv \{M\}$. [The $n' = n$ term in the sum of Eq. (2.14) contributes to the transition matrix element relevant to some spin-exciton relaxation processes.]

The hybridized states (2.13) and (2.14) diagonalize the first three terms of the Hamiltonian (2.1) to the first order in hyperfine coupling. Correspondingly, these have energies $E_{\rm x}(q)$ and 0 (counted from the energy of the $|\{M\},0\rangle$ state) within the approximation neglecting energy corrections of the second order in hyperfine coupling and small magnetic energy corrections related to changes of M_n momenta.

C. Electron-phonon interaction in the exciton representation

The Hamiltonian of the interaction of electrons with 3D acoustic phonons is written as[31]

$$\hat{H}_{e-\rm ph} = \frac{\hbar^{1/2}}{LL_z^{1/2}} \sum_{\mathbf{q},k_z,s} U'_s(\mathbf{k})\,\hat{P}_{\mathbf{k},s}\mathcal{H}_{e-\rm ph}(\mathbf{q}) + \text{H.c.}, \quad (2.15)$$

where $L^2 = 2\pi\mathcal{N}_\phi l_B^2$ is the 2D area and L_z is the dimension of the sample along $\hat{z}$,

$$\mathcal{H}_{e-\rm ph}(\mathbf{q}) = \int e^{i\mathbf{qr}}\hat{\Psi}^\dagger(\mathbf{r})\hat{\Psi}(\mathbf{r})\,d^2r, \quad \mathbf{k} = (\mathbf{q},k_z); \quad (2.16)$$

where $\hat{P}_{\mathbf{k},s}$ is the phonon annihilation operator (index s denotes possible phonon polarizations: the longitudinal l or one of the two transverse polarizations t_1 or t_2), and $U'_s(\mathbf{k})$ is the renormalized vertex which includes the fields of deformation (DA) and piezoelectric (PA) interactions. The integration with respect to z has been already performed and leads to the renormalization $U'_s(\mathbf{k}) = U_s(\mathbf{k})\int \chi^*(z)e^{ik_z z}\chi(z)\,dz$.

The isotropic model for the phonon field[32] enables us to take into account the deformation and piezoelectric couplings independently. We further use the approximation where we take no difference between longitudinal and transverse sound velocities. For the three-dimensional (3D) vertex one needs only the expressions for the squares,[31,32]

$$|U_s|^2 = \pi\varepsilon_{\rm ph}(\mathbf{k})/p_0^3\tau_s(\mathbf{k}), \quad (2.17)$$

where the phonon energy is $\varepsilon_{\rm ph} = \hbar c\sqrt{k_z^2 + q^2}/l_B$ (we recall that k_z and $\mathbf{q}$ are dimensionless), $p_0 = 2.52 \times 10^6$ cm^{-1} is the material parameter of GaAs (see Ref. 32). The longitudinal $\tau_l(\mathbf{k})$ and transverse $\tau_t(\mathbf{k})$ times are the 3D acoustic phonon lifetimes (see Appendix A). These quantities are expressed in terms of nominal times τ_D and τ_P characterizing, respectively, DA and PA phonon scattering in three-dimensional GaAs crystal (see Appendix A and Ref. 20 and cf. Ref. 32).

The dimensionless operator $\mathcal{H}_{e-\rm ph}$ in terms of the excitonic representation has the following simple form (cf. Ref. 33):

$$\mathcal{H}_{e-\rm ph}(\mathbf{q}) = f(q)\mathcal{N}_\phi(\mathcal{A}_{\mathbf{q}} + \mathcal{B}_{\mathbf{q}}). \quad (2.18)$$

D. The spin-orbit coupling in the excitonic representation

If considering the spin-orbit coupling, we will ignore the hyperfine coupling but take into account the $H_{\rm so}$ operator in the single-electron part $\hat{H}_1$ of the Hamiltonian [Eq. (2.1)]:

$$\hat{H}_{\rm so} = \alpha(\hat{\mathbf{q}} \times \hat{\boldsymbol{\sigma}})_z + \beta(\hat{q}_y\hat{\sigma}_y - \hat{q}_x\hat{\sigma}_x), \quad \hat{\mathbf{q}} = -i\nabla + e\mathbf{A}/c\hbar. \quad (2.19)$$

This operator, specified for the (001) GaAs plane represents a combination of the Rashba term ($\sim\alpha$) and the crystalline anisotropy term ($\sim\beta$)[34] and does not violate translational symmetry.[35]

Now it is convenient to use a bare single-electron basis diagonalizing Hamiltonian $\hat{\mathbf{q}}^2/2m_e^* + H_{\rm so}$. To within the leading order in the $H_{\rm so}$ terms we obtain

$$\Psi_{pa} = \begin{pmatrix} \psi_{np} \\ v\sqrt{n+1}\psi_{n+1\,p} + iu\sqrt{n}\psi_{n-1\,p} \end{pmatrix} \quad \text{and} \quad \Psi_{pb} = \begin{pmatrix} -v\sqrt{n}\psi_{n-1\,p} + iu\sqrt{n+1}\psi_{n+1\,p} \\ \psi_{np} \end{pmatrix}, \tag{2.20}$$

where u and v are small dimensionless parameters: $u = \beta\sqrt{2}/l_B\hbar\omega_c$ and $v = \alpha\sqrt{2}/l_B\hbar\omega_c$. Thus the single-electron states acquire a chirality a or b instead of spin quantum number, and the spin flip corresponds to the $a \to b$ process. The definition of the spin-exciton creation operator formally remains the same [Eq. (2.2)]; however, the a_p and b_p operators describe annihilation in the states (2.20) now.

When being presented in terms of basis states (2.20), spin operators $\int \Psi^\dagger \hat{\mathbf{S}}^2 \Psi d^2\mathbf{r}$ and $\int \Psi^\dagger \hat{S}_z \Psi d^2\mathbf{r}$ [where $\Psi = \sum_p (a_p\Psi_{pa} + b_p\Psi_{pb})$] are invariant up to the second order of u and v. However, in the excitonic representation the interaction Hamiltonian $\hat{H}_{\rm int}$ and the electron-phonon coupling operator acquire terms proportional to u and v, which are additional to Eqs. (2.5) and (2.18), respectively.[19–21,33] These terms correspond to creation and annihilation of spin excitons in the system:

$$\hat{H}'_{\rm int} = \mathcal{N}_\phi^{1/2} \sum_{\mathbf{q}} (iuq_+ - vq_-) W(q) (\mathcal{A}^\dagger_{\mathbf{q}} + \mathcal{B}^\dagger_{\mathbf{q}}) \mathcal{Q}_{\mathbf{q}} + \text{H.c.} \tag{2.21}$$

and

$$\mathcal{H}'_{\rm e-ph}(\mathbf{q}) = \mathcal{N}_\phi^{1/2} f(q) (iuq_+ - vq_-) \mathcal{Q}_{\mathbf{q}} + \text{H.c.} \tag{2.22}$$

[$q^\pm = \mp i(q_x \pm iq_y)/\sqrt{2}$].

We can also take into account the presence of an external smooth random potential $\varphi(\mathbf{r})$. This is assumed to be Gaussian and defined by a correlator $K(\mathbf{r}) = \langle \varphi(\mathbf{r})\varphi(0)\rangle$. By choosing $\langle\varphi(\mathbf{r})\rangle = 0$, the correlator is $K(\mathbf{r}) = \Delta^2 \exp(-r^2/\Lambda^2)$, in terms of the correlation length Λ and the amplitude Δ. The smooth random potential can act as the rate-limiting process in the energy dissipation which makes the spin-flip process irreversible. $\varphi(\mathbf{r})$ formally is analogous to frozen field of phonons having zero frequency. A static potential cannot cause dissipation alone: physically the random potential (mixed with the spin-orbit term) causes spin-flip and breaks momentum conservation. The actual dissipation comes from other interactions that do not change the spin: electron-electron and electron-phonon interactions that occur on a faster time scale and render the process irreversible. Therefore, using again the Eq. (2.20) basis set and Eq. (2.10), we obtain the $\hat{\varphi}$ operator in terms of the excitonic representation. The part responsible for a spin flip is [14,17]

$$\hat{\varphi}' = \mathcal{N}_\phi^{1/2} \sum_{\mathbf{q}} f(q)\overline{\varphi}(\mathbf{q})(iuq_+ - vq_-)\mathcal{Q}_{\mathbf{q}} + \text{H.c.}, \tag{2.23}$$

where $\overline{\varphi}$ is the Fourier component [$\varphi(\mathbf{r}) = \sum_{\mathbf{q}} \overline{\varphi}(\mathbf{q}) e^{i\mathbf{qr}}$].

III. THE SPIN-EXCITON–SPIN-EXCITON SCATTERING RELAXATION CHANNELS GOVERNED BY THE HYPERFINE COUPLING

The $\delta S_z = -1$ hybridized states [Eqs. (2.13) and (2.14)] diagonalize the Hamiltonian $\hat{H}_{\rm int} + \hat{H}_{\rm hf}$, but the $\delta S_z = -2$ states $\mathcal{Q}^\dagger_{\mathbf{q}_1}|\text{SE},\mathbf{q}_2\rangle$ and $\mathcal{Q}^\dagger_{\mathbf{q}}|\text{NST},n\rangle$ do not. (Here by S_z we mean the total spin number of the combined nuclear and electron system.) The problem may be formulated in terms of a scattering where the double-exciton state $\mathcal{Q}^\dagger_{\mathbf{q}_1}|\text{SE},\mathbf{q}_2\rangle$ transforms to the single-exciton one $\mathcal{Q}^\dagger_{\mathbf{q}}|\text{NST},n\rangle$. Since the hyperfine coupling energy is neglected, the energy conservation law takes the form

$$E_x(q_1) + E_x(q_2) = E_x(q). \tag{3.1}$$

It determines the modulus of the spin-exciton momentum $\mathbf{q}$ in the final state and, in particular, means that $\mathbf{q}$ cannot be equal to $\mathbf{q}_1$ or $\mathbf{q}_2$.

A. Kinematic scattering

The transition matrix element $\mathcal{M}_{if}$ in Eq. (1.4) has to be found to first order in the hyperfine coupling. Therefore, in the case of the kinematic scattering, where $\mathcal{M}_{if}$ represents an expectation value $\langle\text{bra}|\hat{H}_{\rm hf}|\text{ket}\rangle$ calculated directly for the hyperfine coupling operator, the ket and bra vectors are determined only by the main components of the $\mathcal{Q}^\dagger_{\mathbf{q}_1}|\text{SE},\mathbf{q}_2\rangle$ and $\mathcal{Q}^\dagger_{\mathbf{q}}|\text{NST},n\rangle$ states without any hyperfine coupling corrections. Namely, taking into account that the initial double-exciton state and the final single-exciton one have to be normalized, we should calculate the kinematic scattering matrix element

$$\mathcal{M}^{\rm kin}_{if}(\mathbf{q}_1,\mathbf{q}_2,\mathbf{q},n) = \langle 0,\{M\}^-_n|\mathcal{Q}_{\mathbf{q}}\hat{H}_{\rm hf}\mathcal{Q}^\dagger_{\mathbf{q}_1}\mathcal{Q}^\dagger_{\mathbf{q}_2}|\{M\},0\rangle/\nu'^{3/2}. \tag{3.2}$$

After substitution of Eqs. (2.11) and (2.12), this is reduced to calculation of the four-operator expectation value [Eq. (C1)] (see Appendix C). Note that were the $\mathcal{Q}$ operators usual Bose operators, the expectation [Eq. (C1)] would simply be equal to $\delta_{\mathbf{q}',\mathbf{q}_1}\delta_{\mathbf{q},\mathbf{q}_2} + \delta_{\mathbf{q}',\mathbf{q}_2}\delta_{\mathbf{q},\mathbf{q}_1}$, the conservation condition (3.1) could not be satisfied, and, therefore, the kinematic scattering channel would not exist. Therefore, *only due to the non-Bose nature of the spin-exciton states does this relaxation mechanism take place.*

We should keep in $\mathcal{M}^{\rm kin}_{if}$ only the main terms contributing to the final result, namely to the relaxation rate calculated on the basis of the Fermi golden rule [Eq. (1.4)] and subsequent summation over the $\mathbf{q}_1$, $\mathbf{q}_2$, and $\mathbf{q}$ statistical distributions. These are terms to the lowest power of q_1, q_2, and q. They give the exact result to leading order in the small parameter TM_x. (T is the temperature, characteristic values of the momenta are $q_1, q_2, q \sim \sqrt{TM_x} \ll 1$.) In particular, one finds that the $\sim v/\mathcal{N}_\phi$ terms in Eq. (C1) give the strongest contribution, and the $\sim\langle 0|\mathcal{A}_{\dots}\mathcal{A}^\dagger_{\dots}|0\rangle$ terms may be neglected.[36] In addition, the terms where $\mathbf{q} = \mathbf{q}_1$ or $\mathbf{q} = \mathbf{q}_2$ are omitted due to the "selection rule" determined by Eq. (3.1). As a result, we obtain

$$\mathcal{M}^{\rm kin}_{if}(\mathbf{q}_1,\mathbf{q}_2,\mathbf{q},n) = -\frac{v_0 A_n |\chi(Z_n)|^2}{2\pi l_B^2}\sqrt{\frac{\left(\frac{3}{2}+M_n\right)\left(\frac{5}{2}-M_n\right)}{\mathcal{N}_\phi^3\nu'}} \times e^{i(\mathbf{q}_1+\mathbf{q}_2-\mathbf{q})\boldsymbol{R}_n}. \tag{3.3}$$

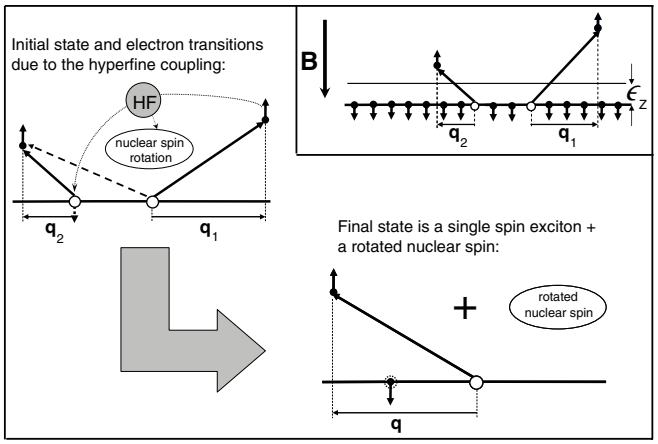

FIG. 2. (Color online) Transitions relevant to calculation of the kinematic scattering matrix element [Eqs. (3.2) and (3.3)]. The initial state is shown in the inset (see text). The magnetic field is assumed to be directed downward (direction of the $\hat{z}$ axis). The hyperfine (HF) vertex is depicted as the gray circle. The dotted line arrow shows the mediated electron transition. Another arrow beginning from the HF vertex marks the transition in the nuclear spin system (change by $\delta I_z = 1$). The final spin-exciton state is shown at the bottom of the figure, where the conventionally annihilated electron and "hole" are also depicted. Background electrons occupying the lowest spin sublevel are drawn *only* in the inset.

Figure 2 indicates schematically electron transitions relevant to the calculated kinematic scattering matrix element. The convention is that horizontal direction in the diagrams represents the conjugate space for states of the degenerate Landau level. The vertical direction is used to indicate the energy of excited states with respect to the ground-state level. The inset represents an initial two-spin-exciton state. (In the figure, as in the following Figs. 3–5, one supposes for simplicity that the filling is $\nu = 1$.) Bold arrows indicate spin excitons, where an electron is promoted from the occupied spin sublevel upward to another spin sublevel of the same Landau level. "Holes" in the occupied sublevel are shown by empty circles. The convention is that excitonic momentum corresponds to distance (along the horizontal axis) from the hole to the excited electron forming the spin exciton. Excited electrons are pictured higher than the Zeeman gap. This reflects the presence of the Coulomb correlation term in the spin-exciton energy [Eq. (1.2)]. To the left of the inset is the diagram for the electron transition in the case of kinematic scattering: due to the hyperfine interaction, an electron annihilates with a hole belonging to another exciton, therefore, one is left with an excited electron and a hole forming the final spin-exciton state depicted by the dashed-line arrow. This single spin exciton has momentum $\mathbf{q}$ (see the final state in Fig. 2), where q must be larger than q_1 and q_2 due to energy conservation [Eq. (3.1)]. {We, again, note that annihilation of the excited electron with its "own" hole, i.e., belonging to the same spin exciton, would result in final exciton with momentum $\mathbf{q}_1$ or $\mathbf{q}_2$, but this forbidden by the same condition [Eq. (3.1)].}

B. Dynamic scattering

If studying the dynamic scattering, one should take into account that the Coulomb interaction operator [Eq. (2.5)], acting on a certain state, does not change the number of the spin-exciton operators determining this state, i.e., this number must be the same in the bra and ket states contributing to $\mathcal{M}_{if} = \langle \text{bra}|\hat{H}_{\text{int}}|\text{ket}\rangle$. Furthermore, the Coulomb interaction does not change the total momentum of the electron gas; it, too, must be the same in the bra and ket states. Therefore, again only the $\sim \mathcal{Q}^\dagger_{\mathbf{q}_1}\mathcal{Q}^\dagger_{\mathbf{q}_2}|\{M\},0\rangle$ component should be kept in the initial state $\mathcal{Q}^\dagger_{\mathbf{q}_1}|\text{SE},\mathbf{q}_2\rangle$. [The hyperfine coupling correction component can contribute only to the transition where $\mathbf{q} = \mathbf{q}_1$, which is forbidden due to Eq. (3.1)].

The single-exciton state $\mathcal{Q}^\dagger_{\mathbf{q}}|0\rangle$ diagonalizes the Hamiltonian $\hat{H}_{\text{int}}$, but the double-exciton state $\mathcal{Q}^\dagger_{\mathbf{q}_1}\mathcal{Q}^\dagger_{\mathbf{q}_2}|0\rangle$ does not. The latter is in fact an "almost" eigenstate. Indeed, even at odd-integer ν we have [cf. Eq. (2.3)]

$$\begin{aligned}&\left[\hat{H}_{\text{int}},\mathcal{Q}^\dagger_{\mathbf{q}_1}\mathcal{Q}^\dagger_{\mathbf{q}_2}\right]|0\rangle\\ &\quad= (\mathcal{E}_{q_1}+\mathcal{E}_{q_2})\mathcal{Q}^\dagger_{\mathbf{q}_1}\mathcal{Q}^\dagger_{\mathbf{q}_2}|0\rangle + \left[\left[\hat{H}_{\text{int}},\mathcal{Q}^\dagger_{\mathbf{q}_1}\right],\mathcal{Q}^\dagger_{\mathbf{q}_2}\right]|0\rangle, \quad (3.4)\end{aligned}$$

where the double-commutation term arises due to the interaction between the spin excitons. It can be routinely calculated with the help of Eqs. (2.4) and (2.5); see Eq. (C2) in Appendix C. The norm of this term and the averaged spin-exciton–spin-exciton interaction energy $\langle 0|\mathcal{Q}_{\mathbf{q}_2}\mathcal{Q}_{\mathbf{q}_1}|[[\hat{H}_{\text{int}},\mathcal{Q}^\dagger_{\mathbf{q}_1}],\mathcal{Q}^\dagger_{\mathbf{q}_2}]|0\rangle$, both vanishing if $q_1 = 0$ or $q_2 = 0$, are, respectively, $\lesssim(\alpha e^2/\kappa l_B)\mathcal{N}_\phi^{-1/2}$ and $\lesssim(\alpha e^2/\kappa l_B)/\mathcal{N}_\phi$ if $q_1 q_2 \neq 0$. The latter estimation quite corresponds to an effective mean dipole-dipole interaction of two spin excitons sized within the area $2\pi l_B^2\mathcal{N}_\phi$. [We recall that each magneto-exciton possesses a dipole momentum equal to $e(\mathbf{q}\times\hat{z})l_B^2$ (in common units).[37]]

It follows from the above that for the dynamic scattering process we choose the ket and bra vectors as

$$\begin{aligned}|\text{ket}\rangle &= \mathcal{Q}^\dagger_{\mathbf{q}_1}\mathcal{Q}^\dagger_{\mathbf{q}_2}|\{M\},0\rangle/\nu', \quad \text{and} \quad \langle\text{bra}| = \langle n,\mathbf{q}|\\ &= -\frac{v_0}{4\pi\sqrt{\nu'\mathcal{N}_\phi}l_B^2}A_n|\chi(Z_n)|^2\sqrt{\left(\frac{3}{2}+M_n\right)\left(\frac{5}{2}-M_n\right)}\\ &\quad\times\langle 0,\{M\}|\mathcal{Q}_{\mathbf{q}}\sum_{\mathbf{q}'}\mathcal{Q}_{\mathbf{q}'}\frac{f(q')}{E_x(q')}e^{i\mathbf{q}'\mathbf{R}_n}, \quad (3.5)\end{aligned}$$

implying that only the hyperfine coupling correction term is relevant in the final normalized state $\mathcal{Q}^\dagger_{\mathbf{q}}|\text{NST},n\rangle/\nu'^{1/2}$. The matrix element meant to be calculated is

$$\mathcal{M}^{\text{dyn}}_{if}(\mathbf{q}_1,\mathbf{q}_2,\mathbf{q},n) = \langle n,\mathbf{q}|\left[\left[\hat{H}_{\text{int}},\mathcal{Q}^\dagger_{\mathbf{q}_1}\right],\mathcal{Q}^\dagger_{\mathbf{q}_2}\right]|\{M\},0\rangle/\nu'. \quad (3.6)$$

Diagrams for the dynamic scattering (Fig. 3) includes vertices of two types: the Coulomb interaction and the hyperfine coupling. In the upper part of Fig. 3 we show schematically an electron transition mediated by the Coulomb interaction and *virtually* converting an initial two-spin-exciton state into another two-spin-exciton state {in accordance with the double-commutation calculation [Eq. (C2)]}. Due to the hyperfine coupling the virtual two-spin-exciton state converts into a single spin exciton via annihilation of an excited electron with an effective hole. Now, in contrast to the kinematic scattering,

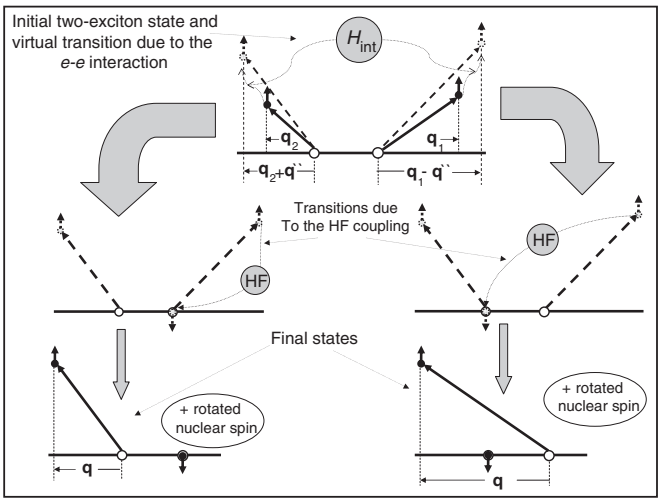

FIG. 3. Diagrams illustrating the dynamic scattering transitions. The initial state and virtual transitions due to the *e-e* Coulomb interaction are shown in the upper part of the figure. Possible annihilation processes are shown in the middle row. The final states are shown in the lower row. (See the text for full details.)

both annihilation processes are allowed: (i) annihilation of an electron with its "own" hole (left diagram in the middle row of Fig. 3) and (ii) with a hole of another spin exciton, similar to the kinematic scattering (right diagram in the middle row). Either transition finally yields a single-spin-exciton state and a change $\delta I_z = 1$ in the nuclear spin system. However, under our conditions, where q_1, q_2, and q are small, contributions of these annihilation transitions to the matrix element [Eq. (3.6)] differ strongly. Indeed, when calculating the matrix element, a key quantity is the expectation value $\langle 0|\mathcal{Q}_{\mathbf{q}}\mathcal{Q}_{\mathbf{q}'}\mathcal{Q}^{\dagger}_{\mathbf{q}_1-\mathbf{q}''}\mathcal{Q}^{\dagger}_{\mathbf{q}_2+\mathbf{q}''}|0\rangle$, with subsequent summation over $\mathbf{q}''$ and $\mathbf{q}'$ in accordance with Eqs. (C2) and (3.5), respectively. This expectation value at $\nu = 1$ and small q_1, q_2, and q consists of two terms: The first is $\delta_{\mathbf{q}',\,\mathbf{q}_1-\mathbf{q}''}\delta_{\mathbf{q},\,\mathbf{q}_2+\mathbf{q}''} + \delta_{\mathbf{q}',\,\mathbf{q}_2+\mathbf{q}''}\delta_{\mathbf{q},\,\mathbf{q}_1-\mathbf{q}''}$, and the second is $-2\mathcal{N}_\phi{}^{-1}\delta_{\mathbf{q}+\mathbf{q}',\,\mathbf{q}_1+\mathbf{q}_2}$ [see Eq. (C1)].[38] The term with two Kronecker deltas, which restricts both summations, contributes to the result with a factor $[W(|\mathbf{q}_1-\mathbf{q}|)+W(|\mathbf{q}_2-\mathbf{q}|)](\mathbf{q}\times\mathbf{q}_1)\cdot(\mathbf{q}\times\mathbf{q}_2)\sim q^3/M_x$, arising due to the action of the two commutation terms in Eq. (3.6) [$W(q)\sim e^2/\kappa l_B q$, see also Eq. (2.7) for definition of the exciton mass]. The second term, independent of $\mathbf{q}''$, maintains a summation over $\mathbf{q}''$, and instead we find $\mathcal{N}_\phi{}^{-1}\sum_{\mathbf{q}''}W(q'')(\mathbf{q}''\times\mathbf{q}_1)(\mathbf{q}''\times\mathbf{q}_2)$, giving a factor $\sim q^2/M_x$. Therefore, the contribution to the matrix element of the first transition is smaller by the multiplicative factor $\sim q\sim\sqrt{TM_x}$.

Therefore, by analogy with the kinematic scattering, we keep in $\mathcal{M}^{\rm dyn}_{if}$ only terms to the lowest power of q_1, q_2, and q. Using sequentially Eqs. (C2), (C1), (2.7), and (3.1), we find

$$\mathcal{M}^{\rm dyn}_{if}(\mathbf{q}_1,\mathbf{q}_2,\mathbf{q},n) = -\frac{\mathbf{q}_1\mathbf{q}_2\,\mathcal{M}^{\rm kin}_{if}(\mathbf{q}_1,\mathbf{q}_2,\mathbf{q},n)}{q^2+\mathbf{q}_1\mathbf{q}_2-\mathbf{q}(\mathbf{q}_1+\mathbf{q}_2)}. \quad (3.7)$$

Both matrix elements Eqs. (3.3) and (3.7) are pertinent to the scattering process shown in Fig. 1(a).

C. The relaxation rate

To calculate the spin-wave relaxation rate, one should know the distribution $N_{\mathbf{q}}$ of spin excitons over the $\mathbf{q}$ wave numbers. Although the exciton operators of Eq. (2.2) are nonbosonic, the spin-excitons obey Bose statistics, because their number in any state determined by a certain $\mathbf{q}$ may, in principle, be macroscopically large. At any moment the spin-exciton distribution is in quasiequilibrium and characterized by a chemical potential $\mu < \epsilon_{\mathbf{Z}}$. (The thermodynamic equilibrium is established much faster than spin-flip processes occur.) Initially, the total number of spin excitons $\mathcal{N}_{\mathbf{x}} = \nu'\mathcal{N}_\phi/2 - S$ is actually determined by a short external optical impulse, and its value might be even more than the critical value

$$\mathcal{N}_{\mathbf{x}c} = \mathcal{N}_\phi\int_{q_0}^{\infty}\frac{qdq}{\exp(\mathcal{E}_q/T)-1} = \mathcal{N}_\phi M_{\rm x}T\left[q_0^2/2M_{\rm x}T - \ln\left(e^{q_0^2/2M_{\rm x}T}-1\right)\right], \quad (3.8)$$

where we have used the quadratic approximation of Eq. (1.3) and designated as q_0 a lowest limit of possible nonzero values of q. Any violation of the translation symmetry contributes to the estimation of q_0. For example, in the ideally clean case $q_0\sim 1/L$, where $L\sim\sqrt{\mathcal{N}_\phi}$ is the linear dimension of the 2D system. A more realistic estimation can be made if one takes into account the presence of a smooth random potential, then $q_0\sim M_x l_B\Delta/\Lambda$, where Δ is the potential amplitude ($\Delta\ll 1/M_x$), and Λ is the correlation length ($\Lambda\gg l_B$).[14] In practice $q_0\lesssim 0.01$. If $\mathcal{N}_x > \mathcal{N}_{xc}$, then the bulk number of spin excitons with nonzero but momenta $|\mathbf{q}|\lesssim q_0$ form a thermodynamic condensate. The specific q distribution of excitons within the condensate plays no role; however, we may write

$$N_{\mathbf{q}} = \begin{cases} N^{\{0\}}_{\mathbf{q}}, & \text{if} \quad \mathbf{q}\in\{0\} \\ 1/[\exp(\mathcal{E}_q/T)-1], & \text{if} \quad \mathbf{q}\notin\{0\} \end{cases} \quad (3.9)$$

($\mathbf{q}\in\{0\}$ means belonging to the thermodynamic condensate). The number of the condensate excitons is, thus, $\mathcal{N}_x - \mathcal{N}_{xc} = \sum_{\mathbf{q}\in\{0\}}N^{\{0\}}_{\mathbf{q}}$. During the spin-exciton relaxation process the condensate is depleted, and when $\mathcal{N}_x < \mathcal{N}_{xc}$ we have

$$N_{\mathbf{q}} = 1/[\exp(\mathcal{E}_q+\epsilon_Z-\mu)/T-1], \quad (3.10)$$

with chemical potential equal to

$$\mu = \epsilon_Z + T\ln\left[1-\exp\left(-\frac{\mathcal{N}_x}{\mathcal{N}_\phi M_x T}\right)\right]. \quad (3.11)$$

[In the vicinity of ϵ_Z the value μ is determined with an accuracy: $|\mu-\epsilon_Z|\gtrsim\min(q_0^2/2M_x, T)$.] The $\mu = 0$ equation determines the equilibrium spin-exciton number: $\mathcal{N}_x^{(0)} = -\mathcal{N}_\phi M_x T\ln(1-e^{-\epsilon_Z/T})$.

The spin-wave relaxation rate is defined as the difference between the fluxes of annihilating and created spin excitons in the phase space:

$$-\frac{d\mathcal{N}_{\mathbf{x}}}{dt} = \frac{1}{2}\sum_{\mathbf{q}_1,\mathbf{q}_2}S(\mathbf{q}_1,\mathbf{q}_2)\big[N_{\mathbf{q}_1}N_{\mathbf{q}_2}(1+N_{12}) - N_{12}\big(1+N_{\mathbf{q}_1}\big)\big(1+N_{\mathbf{q}_2}\big)\big], \quad (3.12)$$

where $N_{12} = 1/[e^{(\mathcal{E}_{q_1}+\mathcal{E}_{q_2}+\epsilon_Z)/T}-1]$ if $\mathcal{N}_x > \mathcal{N}_{xc}$ or $N_{12} = 1/[e^{(\mathcal{E}_{q_1}+\mathcal{E}_{q_2}+2\epsilon_Z-\mu)/T}-1]$ if $\mathcal{N}_x < \mathcal{N}_{xc}$, and the summation

over final-state values $\mathbf{q}$ is performed by calculating

$$S(\mathbf{q}_1,\mathbf{q}_2) = \frac{2\pi}{\hbar}\sum_n\sum_{\mathbf{q}}\left|\mathcal{M}_{if}^{\rm kin}(\mathbf{q}_1,\mathbf{q}_2,\mathbf{q},n)+\mathcal{M}_{if}^{\rm dyn}(\mathbf{q}_1,\mathbf{q}_2,\mathbf{q},n)\right|^2\delta(\mathcal{E}_q-\mathcal{E}_{q_1}-\mathcal{E}_{q_2}-\epsilon_Z)$$
$$= \frac{v_0^2 M_x\left[1+\mathcal{F}\left(q_1^2,q_2^2,\phi,2M_x\epsilon_Z\right)\right]}{2\pi\mathcal{N}_\phi^2\hbar\nu' l_B^4}\sum_n\left(\frac{3}{2}+M_n\right)\left(\frac{5}{2}-M_n\right)A_n^2|\chi(Z_n)|^4 = \left[1+\mathcal{F}\left(q_1^2,q_2^2,\phi,2M_x\epsilon_x\right)\right]/\mathcal{N}_\phi\tau_{\rm hf}, \tag{3.13}$$

where ϕ is the angle between $\mathbf{q}_1$ and $\mathbf{q}_2$,

$$\mathcal{F}(x,y,\phi,\beta) = \frac{xy\cos^2\phi\,(\beta+x+y)}{[\beta^2+\beta(x+y)+xy\cos^2\phi]^{3/2}} \quad \text{and} \tag{3.14}$$

$$\frac{1}{\tau_{\rm hf}} = \frac{5v_0M_x\left(A_{\rm Ga}^2+A_{\rm As}^2\right)}{2d\hbar\nu' l_B^2} \tag{3.15}$$

[we have kept in $\mathcal{F}$ only terms nonvanishing after averaging over the $\mathbf{q}_1$ and $\mathbf{q}_2$ directions when in Eq. (3.12)]. The summation over n in Eq. (3.12) has been performed for the case of unpolarized nuclei. In addition, the correlation length of the spatial nuclear momenta distribution has been considered to be smaller than the magnetic length l_B and conventional width of the two-dimensional electron gas: $d = (\int|\chi(z)|^4dz)^{-1}$. (This value is certainly not equal to the quantum well width $d_{\rm QW}$ but constitutes a fraction of it, e.g., $d/d_{\rm QW}\simeq 1/3$.)

The rate $-d\mathcal{N}_x/dt$ is completely determined by Eqs. (3.9)–(3.15). In the following calculations we use the following: (i) the kinematic and dynamic scattering fluxes simply add, as independent contributions to the total rate; (ii) in the case of $T\ll\epsilon_Z$, the contribution to the rate due to the dynamic scattering relaxation flux is negligibly small; the same result is found if one of spin excitons in the initial state belongs to the thermodynamic condensate (i.e., $\mathbf{q}_1$ or/and $\mathbf{q}_2\in\{0\}$); and (iii) $S(\mathbf{q}_1,\mathbf{q}_2)$ does not depend on $\mathbf{q}_1$ and $\mathbf{q}_2$ for kinematic scattering and the summation in Eq. (3.12) reduces to

$$\sum_{\mathbf{q}_1,\mathbf{q}_2}[\cdots] = \mathcal{N}_x^2 - \sum_{\mathbf{q}_1,\mathbf{q}_2}N_{12}\left(1+N_{\mathbf{q}_1}+N_{\mathbf{q}_2}\right). \tag{3.16}$$

In the $T\gtrsim\epsilon_Z$ region the spin-orbit relaxation channels are much more intense than the considered hyperfine coupling channel (see the next sections), and both spin-orbit and hyperfine coupling relaxation mechanisms compete with each other only in the $T\ll\epsilon_Z$ case. Therefore, we specifically study this situation. The dynamic spin-exciton–spin-exciton scattering then is neglected, and the spin-exciton creation term in Eq. (3.16) may be presented as $-\sum_{\mathbf{q}_1,\mathbf{q}_2}N_{12}(\cdots)\approx -e^{-\mu/T}\sum_{\mathbf{q}_1,\mathbf{q}_2}N_{\mathbf{q}_1}N_{\mathbf{q}_2}(1+N_{\mathbf{q}_1}+N_{\mathbf{q}_2})/(1+N_{\mathbf{q}_1})(1+N_{\mathbf{q}_2})$. In the $\mu\gg T$ case this term is a negligible quantity compared to $\mathcal{N}_x^2$. If we consider $\mu\lesssim T$, then the term is equal to $-\mathcal{N}_x\mathcal{N}_x^{(0)}$. So, if $T\ll\epsilon_Z$, then for any relation between μ and T one finds that Eq. (3.12) reduces to

$$-dn_x/dt = n_x\left[n_x-n_x^{(0)}\right]/2\tau_{\rm hf}\quad(T\ll\epsilon_Z) \tag{3.17}$$

[$n_x(t)=\mathcal{N}_x(t)/\mathcal{N}_\phi$ and $n_x^{(0)}=\mathcal{N}_x^{(0)}/\mathcal{N}_\phi$ to note the spin-exciton concentrations]. In fact, under the conditions considered, the observable relaxation process is completed while still $n_x^{(0)}t/2\tau_{\rm hf}\ll 1$, then

$$n_x(t) = \frac{n_x(0)}{1+n_x(0)t/2\tau_{\rm hf}}\,. \tag{3.18}$$

This law is independent of the temperature but depends on the magnitude of the initial spin excitation $n_x(0)$. The effective relaxation rate is $\sim n_x(0)/2\tau_{\rm hf}\lesssim 0.1/\tau_{\rm hf}$ (if one assumes that $n_x(0)\lesssim 0.1$).

D. Role of the interaction of spin excitons with acoustic phonons

In principle, the spin-exciton–phonon coupling mechanism participates both in the spin-exciton–spin-exciton annihilation scattering and in the single-spin-exciton one. However, in the case of spin-exciton–spin-exciton scattering this relaxation channel represents only a small correction to those studied in the previous subsections, proportional to electron-lattice coupling constants. Let us estimate the spin-exciton–phonon relaxation governed by the single-exciton annihilation mechanism. We need to calculate the transition matrix element $\mathcal{M}_{x-{\rm ph}}$ between the state $|{\rm ket}\rangle = |{\rm SE},\mathbf{q}_1\rangle$ and some of final states $|{\rm bra}\rangle = \hat{P}^\dagger_{\mathbf{k},s}|{\rm NST},n\rangle$ for the exciton-phonon operator determined by Eqs. (2.15) and (2.18). Now the energy conservation law reads $E_{\mathbf{x}}(\mathbf{q}_1)=\hbar ck/l_B$, where $\mathbf{k}=(k_z,\mathbf{q})$. Meanwhile, the $\mathbf{q}=0$ phonons do not contribute to the relaxation process, because action of the $\mathcal{H}_{e-{\rm ph}}(0)$ operator in Eq. (2.18) on the $|{\rm SE},0\rangle$ state is reduced to multiplication by a constant—hence, $\mathcal{M}_{x-{\rm ph}}\equiv 0$ due to orthogonality of the $|{\rm SE},\mathbf{q}_1\rangle$ and $|{\rm NST},n\rangle$ states. If $q\neq 0$, then the contribution to $\mathcal{M}_{x-{\rm ph}}$ is determined only by the first component of the ket state $|{\rm SE},\mathbf{q}_1\rangle$, namely by commutators $[\mathcal{H}_{e-{\rm ph}}(\mathbf{q}),\mathcal{Q}^\dagger_{\mathbf{q}_1}]|\{M\},0\rangle/\sqrt{\nu'}$. The latter according to Eq. (2.16) and commutation rules [Eq. (2.4)] vanish in case $\mathbf{q}_1=0$ being proportional to $\mathbf{q}\times\mathbf{q}_1$ at small q_1. This issue is a key point: The matrix element squared $|\mathcal{M}_{x-{\rm ph}}(\mathbf{q}_1)|^2$ is proportional not only to the small constants of the hyperfine coupling and electron-phonon coupling but also to the temperature (more exactly, to the small dimensionless parameter M_xT). As a result, making computations similar to those made above, we finally obtain a relaxation rate linear in n_x: $-d\Delta n_x/dt=\Delta n_x/\tau_{{\rm hf}-{\rm ph}}$ [Δn_x to note the difference $n_x-n_x^{(0)}$], with the characteristic inverse time

$$\frac{1}{\tau_{{\rm hf}-{\rm ph}}}\sim\frac{\nu' v_0 M_x^3\left(A_{\rm Ga}^2+A_{\rm As}^2\right)\epsilon_Z T}{\hbar c l_B^4 d p_0^3\tau_D}. \tag{3.19}$$

(under the considered conditions predominantly the deformation part of the e-phonon coupling contributes to the result). This value is much smaller than the inverse time given by the formula in Eq. (3.15). Much more important is comparison with another value governing also the single-spin-exciton

relaxation process related to phonon emission: namely a certain characteristic inverse time $1/\tau_{\mathrm{so-ph}}$ can be calculated in the case where spin nonconservation instead of the hyperfine coupling is determined by the spin-orbit coupling.[20,21] It is found that at any parameters $1/\tau_{\mathrm{so-ph}}$ is much larger than $1/\tau_{\mathrm{hf-ph}}$ (by two or three orders of magnitude). We conclude that spin-exciton relaxation channels appearing due to the hyperfine coupling together with electron-phonon coupling are very slow and may always be neglected.

IV. THE SPIN-ORBIT RELAXATION CHANNELS

The spin-orbit relaxation channels, similarly to the hyperfine coupling mechanisms, may be subdivided into the two spin-exciton scattering channels and the single-spin-exciton ones. Among them there is a strong spin-exciton–spin-exciton scattering process actually responsible for the spin-exciton relaxation under the conditions of published experimental studies,[6,7] namely at $T \sim 1$ K and $B < 10$ T. This is the spin-exciton–spin-exciton dynamic scattering where the spin flip is determined by the transition matrix element $\langle \mathrm{fin}|\hat{H}'_{\mathrm{int}}|\mathrm{ini}\rangle$ calculated for the operator in Eq. (2.21) and states $|\mathrm{ini}\rangle = \mathcal{Q}^{\dagger}_{\mathbf{q}_1}\mathcal{Q}^{\dagger}_{\mathbf{q}_2}|0\rangle/\nu'$ and $|\mathrm{fin}\rangle = \mathcal{Q}^{\dagger}_{\mathbf{q}}|0\rangle/\sqrt{\nu'}$. Being constrained by energy $E(\mathbf{q}_1) + E(\mathbf{q}_2) = E(\mathbf{q})$ and momentum conservation $\mathbf{q}_1 + \mathbf{q}_2 = \mathbf{q}$, this process occurs if $\mathbf{q}_1\mathbf{q}_2 = \epsilon_Z M_x$; i.e., the phase volume of the scattered spin excitons is essentially restricted. In particular, if the scattering spin excitons belong to the thermodynamic condensate, this relaxation mechanism is switched off. In fact, the dynamic relaxation channel works well only when $T \gtrsim \epsilon_Z$, giving the relaxation time ~ 10 ns.[17,21,39] However, if $T \ll \epsilon_Z$, the characteristic time is drastically extended, as it is proportional to the double exponent $\sim e^{2\epsilon_Z/T}$ (see Ref. 21). Therefore, studying exactly the $T \ll \epsilon_Z$ case where the spin-orbit and hyperfine coupling relaxations are competing, we consider that the spin-exciton–spin-exciton kinematic processes provide more intense relaxation. In the excitonic representation these are determined by operators of Eqs. (2.22) and (2.23) that do not conserve the number of spin excitons.

A. Relaxation via a smooth random potential

The spin-orbit relaxation channel in presence of a smooth random potential is, again, governed by the kinetic equation (3.12) with $S(\mathbf{q}_1,\mathbf{q}_2) = (2\pi/\hbar)\sum_{\mathbf{q}}|\mathcal{M}^{\mathrm{srp}}_{if}(\mathbf{q}_1,\mathbf{q}_2,\mathbf{q})|^2\delta(\mathcal{E}_q - \mathcal{E}_{q_1} - \mathcal{E}_{q_2} - \epsilon_Z)$, where $\mathcal{M}^{\mathrm{srp}}_{if} = \langle \mathrm{fin}|\hat{\varphi}'|\mathrm{ini}\rangle$ and the initial and final states are $|\mathrm{ini}\rangle = \mathcal{Q}^{\dagger}_{\mathbf{q}_1}\mathcal{Q}^{\dagger}_{\mathbf{q}_2}|0\rangle/\nu'$ and $|\mathrm{fin}\rangle = \mathcal{Q}^{\dagger}_{\mathbf{q}}|0\rangle/\sqrt{\nu'}$, respectively. This matrix element corresponds to the elementary process shown in Fig. 1(b). Diagrams illustrating the electron transitions are presented in Fig. 4. In the upper part of the figure a vertical dotted arrow shows *virtual* promotion of the electron from the initial state to the next Landau level with spin flip. This vertical transition, mediated by the spin-orbit coupling that conserves the spin-exciton momentum,[35] forms a virtual cyclotron magnetoplasmon [see the outlined arrow in Fig. 1(b)]. Another transition occurs due to the smooth random potential and results in annihilation of the virtually promoted electron with hole of another exciton. The result is shown by the dashed line arrow and in the lower part of the figure.

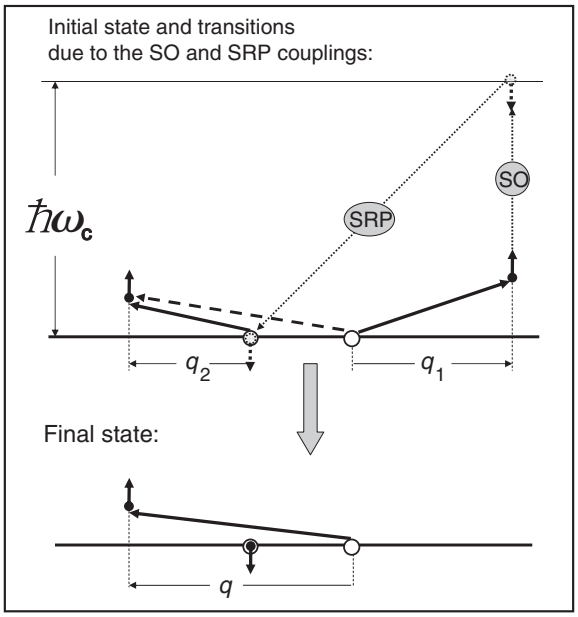

FIG. 4. Diagrams illustrating transitions in the case of the kinematic scattering mediated by the the spin-orbit (SO) couplings and a smooth random potential (SRP). The final state is shown in the lower part of the figure. (See the text for details.)

Taking into account that $\mathcal{E}_{q_1}, \mathcal{E}_{q_2} \ll \epsilon_Z$, the argument of the δ function may be set by $\mathcal{E}_q - \epsilon_Z$, and, using Eq. (C1), we obtain the squared matrix element $|\mathcal{M}^{\mathrm{srp}}_{if}|^2 = 2(u^2 + v^2)|q^*\overline{\varphi}(\mathbf{q}^*)|^2/\nu' N_\phi^2$, where $q^* = \sqrt{2M_x\epsilon_Z}$, and the scattering probability independent of $\mathbf{q}_1$ and $\mathbf{q}_2$: $S = 1/\mathcal{N}_\phi\tau^{\mathrm{srp}}_{\mathrm{so}}$.

The characteristic inverse relaxation time is

$$1/\tau^{\mathrm{srp}}_{\mathrm{so}} = 16\pi^2(u^2 + v^2)M_x^2\epsilon_Z\overline{K}(q^*)/\nu'\hbar\,. \tag{4.1}$$

Here $\overline{K}(q)$ stands for the Fourier component of the correlator. If the latter represents a Gaussian function (see Sec. II D), then $\overline{K}(q^*) = \pi\Delta^2\exp(-M_x\epsilon_Z\Lambda^2/2l_B^2)$.[40] We note that it depends exponentially on the magnetic field squared: $\sim e^{-\gamma B^2}$ (the spin-exciton mass is assumed to be independent of B). As mentioned earlier, this time is assumed to be much longer than the times of thermalization and, therefore, determines the relaxation while the irreversibility occurs due to the fast thermalization. The relaxation rate can then be calculated as in Sec. III C. Independently of whether the thermodynamic condensate exists or not, the rate is governed by equation

$$-dn_x/dt = n_x\left[n_x - n_x^{(0)}\right]/2\tau^{\mathrm{srp}}_{\mathrm{so}}, \tag{4.2}$$

differing from Eq. (3.17) only by the replacement of τ_{hf} with $\tau^{\mathrm{srp}}_{\mathrm{so}}$. Likewise, one obtains Eq. (3.18) by use of the same substitution.

B. Electron-phonon coupling mechanism of the dissipation

We study in this subsection the spin-exciton–spin-exciton scattering process, where there are two spin excitons in the initial state and a single spin exciton plus an emitted phonon in the final state. (For a discussion of single-spin-exciton annihilation due to phonon emission; see comments at the end of Sec. III D). In this case, the conservation laws

read

$$\begin{aligned} \mathbf{q_1}+\mathbf{q_2}&=\mathbf{q}+\mathbf{q}_{\rm ph} \quad \text{and} \\ E(\mathbf{q}_1)+E(\mathbf{q}_2)&=E(\mathbf{q})+\hbar c\sqrt{k_z^2+q_{\rm ph}^2}. \end{aligned} \tag{4.3}$$

Now the kinetic equation for annihilated and created spin excitons is

$$\begin{aligned} -\frac{d\mathcal{N}_{\mathbf{x}}}{dt}=\frac{1}{2}\sum_{\mathbf{q}_1,\mathbf{q}_2,\mathbf{q}} S(\mathbf{q}_1,\mathbf{q}_2,\mathbf{q})\big[N_{\mathbf{q}_1}N_{\mathbf{q}_2}(1+N_{\mathbf{q}}+N_{\rm ph}) \\ -N_{\mathbf{q}}N_{\rm ph}\big(1+N_{\mathbf{q}_1}+N_{\mathbf{q}_2}\big)\big]. \end{aligned} \tag{4.4}$$

Due to the $T \ll \epsilon_Z$ condition we can neglect values $\mathcal{E}_{q_1}$ and $\mathcal{E}_{q_2}$ in the $E(\mathbf{q}_1)+E(\mathbf{q}_2)-E(\mathbf{q})-\varepsilon_{\rm ph}$ argument of the δ function when calculating the scattering probability; therefore,

$$\begin{aligned} S(\mathbf{q}_1,\mathbf{q}_2,\mathbf{q})=\frac{2\pi}{\hbar}\sum_{k_z,\mathbf{q}_{\rm ph},s}|\mathcal{M}_{x-{\rm ph}}(\mathbf{q}_1,\mathbf{q}_2,\mathbf{q},k_z,\mathbf{q}_{\rm ph},s)|^2 \\ \times\delta\big(\epsilon_Z-\mathcal{E}_q-\hbar c\sqrt{k_z^2+q_{\rm ph}^2}\big). \end{aligned} \tag{4.5}$$

The matrix element is $\mathcal{M}_{x-{\rm ph}}=\langle{\rm fin}|\hat{H}_{e-{\rm ph}}|{\rm ini}\rangle$, where the electron-phonon Hamiltonian is presented by Eqs. (2.15)–(2.17) [with change from $\mathcal{H}_{e-{\rm ph}}$ to $\mathcal{H}'_{e-{\rm ph}}$; see Eq. (2.22)] and the bra and ket vectors are $|{\rm fin}\rangle=\hat{P}^\dagger_{k_z,\mathbf{q}_{\rm ph},s}\mathcal{Q}^\dagger_{\mathbf{q}}|0\rangle/\sqrt{\nu'}$ and $|{\rm ini}\rangle=\mathcal{Q}^\dagger_{\mathbf{q}_1}\mathcal{Q}^\dagger_{\mathbf{q}_2}|0\rangle/\nu'$, respectively.

Electron transitions for the $\mathcal{M}_{x-{\rm ph}}$ matrix element are illustrated in Fig. 5. As in Fig. 4, a vertical transition (vertical dotted arrow) occurs due to the spin-orbit (SO) coupling, resulting in a virtual cyclotron magnetoplasmon [see also Fig. 1(c)]. Now the transition to a spin-exciton state (the dashed-line arrow) is via the electron-phonon (e-ph) coupling (the sloping dotted line). In the calculation we use Eq. (C1) and, again, keep only terms $\sim\nu'/\mathcal{N}_\phi$ contributing to the result

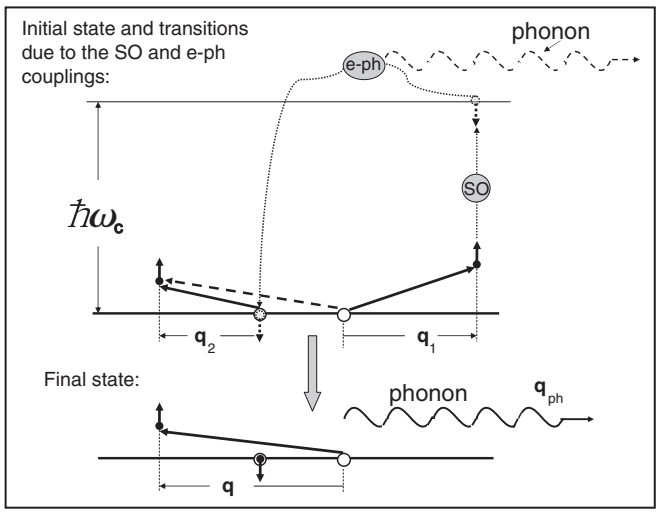

FIG. 5. Electron transitions of the spin-orbit (SO) and electron-phonon (e-ph) scattering. The e-ph coupling plays the same role as the smooth random potential in Fig. 4. The emitted phonon is depicted by a wavy arrow. Now conservation takes place for both energy and momenta: see Eq. (4.3) of the text.

in the leading approximation. Finally, in the same spirit as before, we obtain the relaxation rate (4.4) in the form

$$-dn_x/dt=n_x\big[n_x-n_x^{(0)}\big]/2\tau_{\rm so}^{e-{\rm ph}}, \tag{4.6}$$

similarly to Eqs. (3.17) and (4.2). Now the temperature-independent constant characterizing the rate is [41]

$$1/\tau_{\rm so}^{e-{\rm ph}}=\frac{4(u^2+v^2)M_x^2\epsilon_Z^3\mathcal{G}\big(M_xc^2\hbar^2/\epsilon_Zl_B^2\big)}{\nu' c\hbar l_B^2p_0^3\tau_D}, \tag{4.7}$$

where

$$\mathcal{G}(\xi)=\int_0^{x_0(\xi)}dx\,x\sqrt{(1-x)^2-2\xi x}$$

$[x_0=1+\xi-\sqrt{\xi^2+2\xi}]$. In the derivation we have set $1/\tau_A\approx 1/\tau_D$, because estimates show that the contribution of the deformation coupling dominates that of polarization under the applicable conditions (cf. Sec. III D). Unlike the characteristic value (4.1), which decreases exponentially with the magnetic field, the inverse time (4.7) grows with B with the power law $\sim B^3$. This increase comes from the ϵ_Z^3 factor in Eq. (4.7), which reflects the increased phase space available from the emission of phonons at high fields.[20]

V. COMPARISON OF THE HYPERFINE COUPLING AND SPIN-ORBIT RELAXATION CHANNELS

Summing up the right-hand sides of Eqs. (3.17), (4.2), and (4.6), we find the total relaxation flux,

$$-dn_x/dt=\big(n_x-n_x^{(0)}\big)\left[\frac{n_{\rm x}}{2}\left(\frac{1}{\tau_{\rm hf}}+\frac{1}{\tau_{\rm so}^{\rm srp}}+\frac{1}{\tau_{\rm so}^{e-{\rm ph}}}\right)\right]. \tag{5.1}$$

As the inverse relaxation time is, in fact, proportional to n_x, we characterize the relaxation process at a substantial initial excitation $n_x(0)$. The latter value experimentally is $\sim$0.1 and, under the assumed conditions $T\lesssim 0.1$ K and $B>10$ T (where the equilibrium concentration $n_x^{(0)}<10^{-4}$), one finds the law $n_x(t)=n_x(0)/[1+n_x(0)t/2\tau_{\rm tot}]$, where

$$\frac{1}{\tau_{\rm tot}}=\frac{1}{\tau_{\rm hf}}+\frac{1}{\tau_{\rm so}^{\rm srp}}+\frac{1}{\tau_{\rm so}^{e-{\rm ph}}}. \tag{5.2}$$

Estimates of the $\tau_{\cdots}$ values are possible if we specify material parameters included in formulas (3.15), (4.1), and (4.7). Some of them have been already given in Secs. II B and II C and in Appendixes A and B. In addition, we consider $c=5\times10^5$ cm/s and $\epsilon_Z=0.0255B$ meV. Other parameters related to modern wide quantum-well structures could be chosen as $u^2+v^2=10^{-3}/B$, $\Lambda=50$ nm, $\Delta=0.3$ meV, and $d=8.1$ nm (here B is assumed to be measured in Teslas; see also estimates in Ref. 17). However, the estimate of the effective spin-exciton mass M_x strongly depends on the finite thickness form factor. There are experimental data where M_x is found at comparatively low magnetic fields: (i) $1/M_x\approx 1.2$ meV at $B=2.27$ T and $\nu=1$ in the 33-nm quantum well[16]; (ii) $1/M_{\rm x}\approx 1.51$ meV at $B=2.69$ T and $\nu=1$ in the 23-nm quantum well[15]; and (iii) $1/M_x\approx 0.44$ meV at $B=2.9$ T and $\nu=1/3$ in the 25-nm quantum well.[11] For these fields characterized by the inequality $l_B>d$, the B dependence should be approximately $1/M_x\sim B^{1/2}$, but in the $l_B<d$ strong-field regime the inverse mass grows much

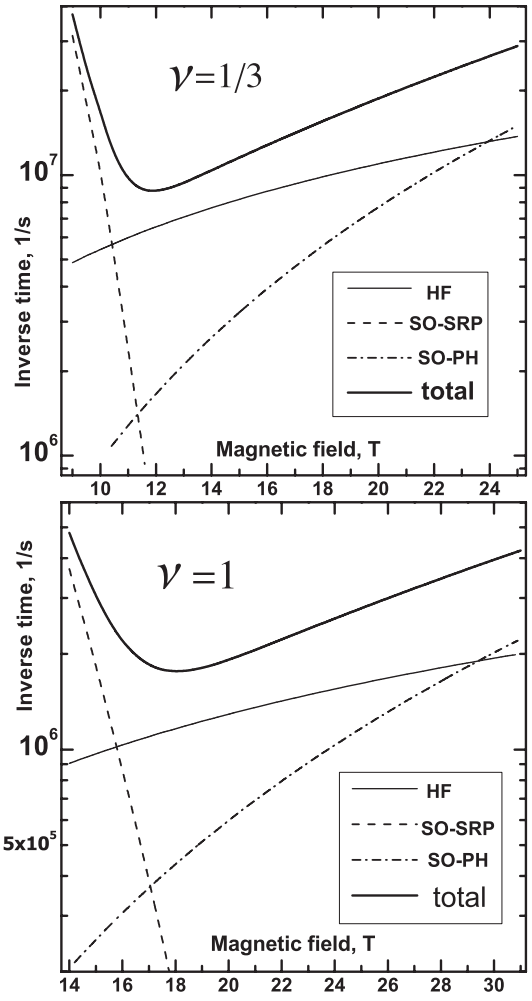

FIG. 6. Calculated inverse relaxation times as a function of magnetic field B from formulas (3.15), (4.1), and (4.7) corresponding to hyperfine, $1/\tau_{\rm hf}$ (solid line); spin-orbit with random potential, $1/\tau_{\rm so}^{\rm srp}$ (dashed line); and spin-orbit with phonon emission, $1/\tau_{\rm so}^{\rm ph}$ (dash-dotted line), respectively. Specific material parameters are given in the text. The bold solid line is the calculated combined inverse time (5.2).

more weakly with B. Based on these data, the semiempirical analysis using characteristic GaAs/AlGaAs form factors allows us to consider values $1/M_x \simeq 2$ meV at $\nu = 1$ and $1/M_x \simeq 0.7$ meV at $\nu = 1/3$ as the characteristic ones for the 10T $< B <$ 25 T range. (Note that at a given field B the estimate $M_x^{-1}|_{\nu<1} \simeq \nu' M_x^{-1}|_{\nu=1}$ holds according to the semiphenomenological theory.[10])

Numerical values of the characteristic inverse relaxation times are plotted in Fig. 6 as a function of the magnetic field. We remark that actual times should be longer by a factor of $\sim 2/n_x(0) \sim$ 20–50 because of the nonexponential solution of Eq. (5.2). The B dependence of the relaxation rate is nonmonotonic. In the region 10 T $< B <$ 30 T the relaxation regime switches twice between the spin-orbit and hyperfine coupling dominance, taking maxima $\simeq$18 T and $\simeq$12 T in the $\nu = 1$ and $\nu = 1/3$ cases, respectively. The reason that the hyperfine interaction becomes dominant is that for increasing magnetic field the nuclei remain disordered, while the random potential is effectively smoothed by the cyclotron motion. At very high fields the spin-orbit interaction again dominates because of the increasing phase space for the emission of phonons. On the basis of these estimates we conclude that the hyperfine coupling relaxation channel should be dominant approximately from 16 to 29 T in the $\nu = 1$ quantum Hall ferromagnet and from 11 to 24 T for $\nu = 1/3$. The latter case would seem to be more accessible to the experimental study of the hyperfine coupling relaxation mechanism, because the usual electron concentrations in GaAs structures do not allow one to attain fields stronger 10 T in the $\nu = 1$ quantum Hall system. We note a feature of the hyperfine coupling relaxation: Its rate is vanishing in the case of spin-polarized nuclei. This should distinguish the hyperfine coupling mechanism from that of the spin orbit and provide a test of the theory. If the nuclear spins could be fully polarized, then only spin-orbit relaxation would be important and there should be crossover between the regime limited by the random potential and the very high field regime of phonon emission. We emphasize also that our results should be valid in immediate vicinity of 1 or 1/3 fillings. Recent experiments show that if ν differs by more than about 0.1 from these special values, one observes a two-mode spectrum of spin excitations—above and below the Zeeman gap.[42] Interaction of these two types of spin waves could considerably accelerate the relaxation.

In conclusion, we have reported on a new spin relaxation mechanism in a spin-polarized strongly correlated two-dimensional electron gas that appears at low temperatures and in strong magnetic fields. This mechanism is related only to the hyperfine coupling with GaAs nuclei and no other interactions are needed for this relaxation channel. The full calculation of relaxation displays a competition of the hyperfine coupling and spin-orbit relaxation processes, which can be summarized by Eqs. (3.15), (4.1), and (4.7). Under the assumed conditions the relaxation process occurs nonexponentially with time. The rate does not depend on temperature but depends on the magnetic field nonmonotonically as can be seen in Fig. 6, which is plotted using estimated material and device parameters taken from experiment. The estimate of the hyperfine relaxation depends on the assumed randomness of the nuclear spins and a test of the theory would be to polarize the nuclear spins.

ACKNOWLEDGMENTS

S.D. thanks the Russian Fund of Basic Research and the LIA Condensed Matter and Theoretical Physics Program (ex ENS-Landau) for support and the Laue Langevin Institute (Grenoble) for hospitality. We are especially grateful to Efim Kats for scientific discussions and suggestions.

APPENDIX A: CALCULATION OF THE HYPERFINE COUPLING PARAMETERS $A_{\rm Ga}$ AND $A_{\rm As}$

We proceed from formula $A_n = (16\pi\mu_B\mu_n/3I_n)|u(\boldsymbol{R}_n)|^2$,[29,30] where μ_n is the nuclear magnetic moment and $u(\boldsymbol{R}_n)$ is the conduction electron Bloch function at the nucleus. $u(\boldsymbol{R})$ is assumed to be normalized as $\int |u(\boldsymbol{R})|^2 d^3R = 1$, where the integration is performed within the GaAs two atom unit cell having volume $v_0 = 45.2$ Å^3. It seems to be the only estimations of $|u(\boldsymbol{R}_{\rm Ga})|^2$ and $|u(\boldsymbol{R}_{\rm As})|^2$ were done in Ref. 28 and subsequently cited by other authors

(cf. Ref. 29). Using these and the μ_n values for As and, for the Ga^{69} and Ga^{71} stable isotopes $\mu_{As} = 1.44$, $\mu_{Ga^{69}} = 2.017$, and $\mu_{Ga^{71}} = 2.56$ (in units of the nuclear magneton $\mu_N = 3.15 \times 10^{-9}$ meV/G),[43] we find $A_{Ga^{69}} \simeq 0.038$ meV, $A_{Ga^{71}} \simeq 0.049$ meV, and $A_{As} \simeq 0.046$ meV. The ratio of the Ga^{69} and Ga^{71} amounts in the semiconductor is considered to be equal to 3:2; therefore, the result is

$$\sum_{\text{within unit cell}} A_n^2 = 0.6(A_{Ga^{69}})^2 + 0.4(A_{Ga^{71}})^2 + (A_{As^{71}})^2 \approx 4 \times 10^{-3}\ \text{meV}^2. \quad \text{(A1)}$$

APPENDIX B: ACOUSTIC PHONON LIFE TIMES τ_l AND τ_t

If we take $\hat{x}$, $\hat{y}$, $\hat{z}$ to be the directions of the principal crystal axes, then for longitudinal phonons we obtain[20,33]

$$\frac{1}{\tau_l(\mathbf{k})} = \frac{1}{\tau_D} + \frac{45 p_0^2}{k^8 \tau_P} q_x^2 q_y^2 k_z^2, \quad \text{(B1)}$$

where

$$\tau_D^{-1} = \frac{\Xi^2 p_0^3}{2\pi\hbar\rho c^2}, \quad \tau_P^{-1} = \left(\frac{e e_{14}}{\kappa}\right)^2 \frac{8\pi p_0}{5\hbar\rho c^2} \quad \text{(B2)}$$

($\mathbf{q}$ and k_z in this appendix are considered to have a common dimension.) Transverse phonons in a cubic crystal do not induce a deformation field.[32] Actually, we need only the inverse time $1/\tau_t$ averaged over all directions of the transverse phonon polarization. If the transverse phonon distribution satisfies the condition that their polarizations are equiprobable, then for either of the two polarization the averaging yields[20,33]

$$\overline{\tau_t^{-1}} = \frac{5 p_0^2}{2k^6 \tau_P}\left(q_x^2 q_y^2 + q^2 k_z^2 - \frac{9 q_x^2 q_y^2 k_z^2}{k^2}\right). \quad \text{(B3)}$$

We have used in Eqs. (B2) and (B3) common notations as follows: $\Xi \simeq 17.5$ eV and $e_{14} \simeq -0.16$ C/m^2 are the relevant deformation potential and piezoelectric constant of the GaAs crystal, $\rho \approx 5.3$ g/cm^2 is the GaAs density, and $\kappa \approx 12.85$ is the dielectric constant. As a result, we find $\tau_D \simeq 0.8$ ps and $\tau_P \simeq 35$ ps.

APPENDIX C

The four-$\mathcal{Q}$-operator expectation value is calculated with the help of Eq. (2.4),

$$\langle 0|\mathcal{Q}_{\mathbf{q}_2'}\mathcal{Q}_{\mathbf{q}_1'}\mathcal{Q}^\dagger_{\mathbf{q}_1}\mathcal{Q}^\dagger_{\mathbf{q}_2}|0\rangle = \delta_{\mathbf{q}_1+\mathbf{q}_2,\,\mathbf{q}_1'+\mathbf{q}_2'}\left[e^{i\phi}\left(\langle 0|\mathcal{A}_{\mathbf{q}_2'-\mathbf{q}_2}\mathcal{A}^\dagger_{\mathbf{q}_1-\mathbf{q}_1'}|0\rangle - \frac{\nu'}{\mathcal{N}_\phi}\right) + e^{-i\phi}\left(\langle 0|\mathcal{A}_{\mathbf{q}_2'-\mathbf{q}_1}\mathcal{A}^\dagger_{\mathbf{q}_2-\mathbf{q}_1'}|0\rangle - \frac{\nu'}{\mathcal{N}_\phi}\right)\right], \quad \text{(C1)}$$

where $\phi = (\mathbf{q}_1' \times \mathbf{q}_1 + \mathbf{q}_2' \times \mathbf{q}_2)_z/2$ and ν' is considered to be equal to ν if $\nu \leqslant 1$ or 1 if the filling factor is an integer. In the important case of integer ν: $\langle 0|\mathcal{A}_{\mathbf{q}}\mathcal{A}^\dagger_{\mathbf{q}}|0\rangle = \delta_{\mathbf{q},0}$. Then, if calculating the matrix element (3.2), the $\langle 0|\mathcal{A}_{\ldots}\mathcal{A}^\dagger_{\ldots}|0\rangle$ terms do not contribute to the probability transition (1.4) due to the energy conservation condition (3.1). This means that the kinematic scattering would be determined only by the double-commutation expectation value $\langle \text{fin}|[[\hat{H}_{\text{hf}}, \mathcal{Q}^\dagger_{\mathbf{q}_1}], \mathcal{Q}^\dagger_{\mathbf{q}_2}]|0\rangle$, similarly to the case of the dynamic scattering, cf. Eq. (3.6).

In Eq. (3.4) the action of the double-commutation term leads to the state

$$\left[\left[\hat{H}_{\text{int}}, \mathcal{Q}^\dagger_{\mathbf{q}_1}\right], \mathcal{Q}^\dagger_{\mathbf{q}_2}\right]|0\rangle = \frac{4}{\mathcal{N}_\phi}\sum_{\mathbf{q}''} W(q'') \sin\left(\frac{\mathbf{q}'' \times \mathbf{q}_1}{2}\right) \times \sin\left(\frac{\mathbf{q}'' \times \mathbf{q}_2}{2}\right)\mathcal{Q}_{\mathbf{q}_1-\mathbf{q}''^\dagger}\mathcal{Q}^\dagger_{\mathbf{q}_2+\mathbf{q}''}|0\rangle. \quad \text{(C2)}$$

[1] B. Tanatar and D. M. Ceperley, Phys. Rev. B **39**, 5005 (1989); S. T. Chui and K. Esfarjani, *ibid.* **44**, 11498 (1991); F. Rapisarda and G. Senatore, Aust. J. Phys. **49**, 161 (1996); see also B. Spivak, S. V. Kravchenko, S. A. Kivelson, and X. P. A. Gao, Rev. Mod. Phys. **82**, 1743 (2010), and publications cited therein.

[2] See, e.g., J. K. Jain, Physics **3**, 71 (2010), and publications cited therein.

[3] A. Pinczuk, B. S. Dennis, D. Heiman, C. Kallin, L. Brey, C. Tejedor, S. Schmitt-Rink, L. N. Pfeiffer, and K. W. West, Phys. Rev. Lett. **68**, 3623 (1992); A. Pinczuk, B. S. Dennis, L. N. Pfeiffer, and K. W. West, *ibid.* **70**, 3983 (1993); Semicond. Sci. Technol. **9**, 1865 (1994).

[4] L. V. Kulik and V. E. Kirpichev, Phys. Usp. **49**, 353 (2006) [Usp. Fiz. Nauk **176**, 365 (2006)].

[5] Yu. A. Nefyodov, A. A. Fortunatov, A. V. Shchepetilnikov, and I. V. Kukushkin, JETP Lett. **91**, 357 (2010).

[6] V. E. Zhitomirskii, V. E. Kirpichev, A. I. Filin, V. B. Timofeev, B. N. Shepel', and K. von Klitzing, JETP Lett. **58**, 439 (1993).

[7] D. Fukuoka, K. Oto, K. Muro, Y. Hirayama, and N. Kumada, Phys. Rev. Lett. **105**, 126802 (2010); D. Fukuoka, T. Yamazaki, N. Tanaka, K. Oto, K. Muro, Y. Hirayama, N. Kumada, and H. Yamaguchi, Phys. Rev. B **78**, 041304(R) (2008).

[8] Yu. A. Bychkov, S. V. Iordanskii, and G. M. Eliashberg, JETP Lett. **33**, 143 (1981); C. Kallin and B. I. Halperin, Phys. Rev. B **30**, 5655 (1984).

[9] S. M. Girvin, A. H. MacDonald, and P. M. Platzman, Phys. Rev. Lett. **54**, 581 (1985); Phys. Rev. B **33**, 2481 (1986).

[10] J. P. Longo and C. Kallin, Phys. Rev. B **47**, 4429 (1993).

[11] I. V. Kukushkin, J. H. Smet, D. S. Lyne Abergel, V. I. Fal'ko, W. Wegscheider, and K. von Klitzing, Phys. Rev. Lett. **96**, 126807 (2006).

[12] A. B. Van'kov, L. V. Kulik, S. Dickmann, I. V. Kukushkin, V. E. Kirpichev, W. Dietsche, and S. Schmult, Phys. Rev. Lett. **102**, 206802 (2009).

[13] L. V. Kulik, S. Dickmann, I. K. Drozdov, A. S. Zhuravlev, V. E. Kirpichev, I. V. Kukushkin, S. Schmult, and W. Dietsche, Phys. Rev. B **79**, 121310(R) (2009).

[14] S. Dickmann, Phys. Rev. Lett. **93**, 206804 (2004).

[15] I. V. Kukushkin, J. H. Smet, V. W. Scarola, V. Umansky, and K. von Klitzing, Science **324**, 1044 (2009) [see the Supporting Online Material: www.sciencemag.org/cgi/content/full/1171472/DC1]

[16] Y. Gallais, J. Yan, A. Pinczuk, L. N. Pfeiffer, and K. W. West, Phys. Rev. Lett. **100**, 086806 (2008).

[17] S. Dickmann and S. L. Artyukhin, JETP Lett. **89**, 133 (2009); see also e-print arXiv:0812.1703.

[18] S. Dickmann, JETP Lett. **93**, 86 (2011).

[19] S. Dickmann and S. V. Iordanskii, JETP Lett. **63**, 50 (1996).

[20] S. Dickmann and S. V. Iordanskii, JETP **83**, 128 (1996).

[21] S. Dickmann and S. V. Iordanskii, JETP Lett. **70**, 543 (1999).

[22] The exciton operators (2.2) were used in the following works for the first time: A. B. Dzyubenko and Yu. E. Lozovik, Sov. Phys. Solid State **25**, 874 (1983); [**26**, 938 (1984)].

[23] Yu. A. Bychkov and S. V. Iordanskii, Sov. Phys. Solid State **29**, 1405 (1987).

[24] S. Dickmann, Phys. Rev. B **65**, 195310 (2002).

[25] S. Dickmann, V. Fleurov, and K. Kikoin, Phys. Rev. B **76**, 205309 (2007).

[26] S. M. Girvin, Phys. Rev. B **29**, 6012 (1984).

[27] L. D. Landau and E. M. Lifshitz, *Quantum Mechanics: Non-Relativistic Theory*, 3rd ed. (Pergamon Press, London, 1977), Vol. 3.

[28] D. Paget, G. Lampel, B. Sapoval, and V. I. Safarov, Phys. Rev. B **15**, 5780 (1977).

[29] M. I. Dyakonov and V. I. Perel, in *Optical Orientation*, edited by B. Meier and B. P. Zakharchenia (North-Holland, Amsterdam, 1984), Ch. II.

[30] I. A. Merkulov, Al. L. Efros, and M. Rosen, Phys. Rev. B **65**, 205309 (2002).

[31] See, e.g., S. V. Iordanskii and B. A. Muzykantskii, JETP **69**, 1006 (1989).

[32] V. F. Gantmakher, and Y. B. Levinson, *Carrier Scattering in Metals and Semiconductors* (North-Holland, Amsterdam, 1987).

[33] S. Dickmann, Phys. Rev. B **61**, 5461 (2000).

[34] Yu. A. Bychkov and E. I. Rashba, JETP Lett. **39**, 78 (1984); M. I. D'yakonov and V. Yu. Kachorovskii, Sov. Phys. Semicond. **20**, 110 (1986).

[35] This feature is evident from the fact that $H_{\rm so}$ commutes with the operator $\hat{\mathbf{P}} = \sum_j [\hbar\hat{\mathbf{q}}_j - (e/c)\mathbf{B}\times\mathbf{r}_j]$. The latter plays the role of total momentum of a magnetized 2DEG considered in the "clean limit" [cf. Ref. 37].

[36] According to Eq. (2.6) and to the g-function calculation,[9,26] the expansion $\langle 0\mathcal{A}_{\mathbf{q}}\mathcal{A}^{\dagger}_{\mathbf{q}}0\rangle = \nu^2\delta_{\mathbf{q},0} + \frac{1-\nu}{\mathcal{N}_\phi}(q^4/8 + \cdots)$, where $\nu \leqslant 1$, takes place at small q.

[37] L. P. Gor'kov and I. E. Dzyaloshinskii, JETP **26**, 449 (1968).

[38] The diagrams in Figs. 3–5 are drawn for the case $\nu = 1$. However, a Hartree-Fock calculation gives similar terms for the four-exciton expectation value (C1); namely the terms in parentheses are $\langle 0|\mathcal{A}_{\mathbf{q}_1}\mathcal{A}^{\dagger}_{\mathbf{q}_2}|0\rangle - \nu'/\mathcal{N}_\phi = -\nu'^2\delta_{\mathbf{q}_1,\mathbf{q}_2}/\mathcal{N}_\phi + \nu'^2\delta_{\mathbf{q}_1,0}\delta_{\mathbf{q}_2,0}$.

[39] This calculation is in satisfactory agreement with experimental data of Refs. 7, where the spin relaxation has been studied if the initial deviation was definitely an excited spin-exciton state. We note that those authors refer to the publication 14, which treated Goldstone mode relaxation, but Refs. 21 and 17 would have been more appropriate.

[40] Formula (4.1) was derived earlier by using a more general approach, wherein the Goldstone mode relaxation was considered.[14] However, during the Goldstone mode relaxation the thermodynamic condensate sequentially increases and decays, and its evolution is also governed by the time (4.1).

[41] The value $\tau_{\rm so}^{e-{\rm ph}}$ is *half* the characteristic relaxation time found for the Goldstone condensate of "zero spin excitons" in the $\xi \to 0$ limit, in the case where it is determined by the spin-orbit and electron-phonon interactions.[19] The cause of this apparent discrepancy lies in the fact that the norm of any coherent state $\mathcal{Q}^{\dagger}_{\mathbf{q}}\mathcal{Q}^{\dagger}_{\mathbf{q}}|0\rangle$ (including the $\mathbf{q} \equiv 0$ case) is equal to 2, but the norm $\langle 0|\mathcal{Q}_{\mathbf{q}_2}\mathcal{Q}_{\mathbf{q}_1}\mathcal{Q}^{\dagger}_{\mathbf{q}_1}\mathcal{Q}^{\dagger}_{\mathbf{q}_2}|0\rangle$ of our ini⟩ state is equal to 1 if calculated for the $\mathbf{q}_1 \neq \mathbf{q}_2$ case. When studying the transition matrix element, the initial state $\mathcal{Q}^{\dagger}_{\mathbf{q}_1}\mathcal{Q}^{\dagger}_{\mathbf{q}_2}|0\rangle$ should be appropriately normalized. However, in our present problem the contribution to the result of the $\mathbf{q}_1 = \mathbf{q}_2$ states is statistically negligible compared with those of $\mathbf{q}_1 \neq \mathbf{q}_2$.

[42] I. K. Drozdov, L. V. Kulik, A. S. Zhuravlev, V. E. Kirpichev, I. V. Kukushkin, S. Schmult, and W. Dietsche, Phys. Rev. Lett. **104**, 136804 (2010).

[43] P. Raghavan, At. Data Nucl. Data Tables **42**, 189 (1989).